

1 **A metanalysis of microcosm experiments shows that dimethyl**
2 **sulfide (DMS) production in polar waters is insensitive to ocean**
3 **acidification**

4 Frances E. Hopkins¹, Philip D. Nightingale¹, John A. Stephens¹, C. Mark Moore², Sophie
5 Richier², Gemma L. Cripps², Stephen D. Archer³

6 ¹Plymouth Marine Laboratory, Plymouth, PL1 3DH, U.K.

7 ²Ocean and Earth Science, National Oceanography Centre, University of Southampton,
8 Southampton, U.K.

9 ³Bigelow Laboratory for Ocean Sciences, Maine, U.S.A.

10 *Correspondence to:* Frances E. Hopkins (fhop@pml.ac.uk)

11 **Abstract.** Emissions of dimethylsulfide (DMS) from the polar oceans play a key role in
12 atmospheric processes and climate. Therefore, it is important to increase our understanding of
13 how DMS production in these regions may respond to climate change. The polar oceans are
14 particularly vulnerable to ocean acidification (OA). However, our understanding of the polar
15 DMS response is limited to two studies conducted in Arctic waters, where in both cases DMS
16 concentrations decreased with increasing acidity. Here, we report on our findings from seven
17 summertime shipboard microcosm experiments undertaken in a variety of locations in the
18 Arctic Ocean and Southern Ocean. These experiments reveal no significant effects of short
19 term OA on the net production of DMS by planktonic communities. This is in contrast to
20 similar experiments from temperate NW European shelf waters where surface ocean
21 communities responded to OA with significant increases in dissolved DMS concentrations. A
22 meta-analysis of the findings from both temperate and polar waters ($n = 18$ experiments)
23 reveals clear regional differences in the DMS response to OA. Based on our findings, we
24 hypothesise that the differences in DMS response between temperate and polar waters reflect
25 the natural variability in carbonate chemistry to which the respective communities of each
26 region may already be adapted. If so, future temperate oceans could be more sensitive to OA

27 resulting in an increase in DMS emissions to the atmosphere, whilst perhaps surprisingly
28 DMS emissions from the polar oceans may remain relatively unchanged. By demonstrating
29 that DMS emissions from geographically distinct regions may vary in their response to OA,
30 our results may facilitate a better understanding of Earth's future climate. Our study suggests
31 that the way in which processes that generate DMS respond to OA may be regionally distinct
32 and this should be taken into account in predicting future DMS emissions and their influence
33 on Earth's climate.

34 **1 Introduction**

35 The trace gas dimethylsulfide (DMS) is a key ingredient in a cocktail of gases that exchange
36 between the ocean and atmosphere. Dissolved DMS is produced via the enzymatic
37 breakdown of dimethylsulfoniopropionate (DMSP), a secondary algal metabolite implicated
38 in a number of cellular roles, including the regulation of carbon and sulfur metabolism via an
39 overflow mechanism (Stefels, 2000) and protection against oxidative stress (Sunda et al.,
40 2002). Oceanic DMS emissions amount to 17 - 34 Tg S y⁻¹, representing 80 - 90% of all
41 marine biogenic S emissions, and up to 50% of global biogenic emissions (Lana et al., 2011).
42 DMS and its oxidation products play vital roles in atmospheric chemistry and climate
43 processes. These processes include aerosol formation pathways that influence the
44 concentration of cloud condensation nuclei (CCN) with implications for Earth's albedo and
45 climate (Charlson et al., 1987; Korhonen et al., 2008a), and the atmospheric oxidation
46 pathways of other key climate gases, including isoprene, ammonia and organohalogenes (Chen
47 and Jang, 2012; von Glasow and Crutzen, 2004; Johnson and Bell, 2008). Thus, our ability to
48 predict the climate into the future requires an understanding of how marine DMS production
49 may respond to global change (Carpenter et al., 2012; Woodhouse et al., 2013; Menzo et al.,
50 2018).

51 The biologically-rich ice-edge regions and open seas of the Arctic are a strong source of
52 DMS to the Arctic atmosphere (Levasseur, 2013). A seasonal cycle in CCN numbers can be
53 related to seasonality in the Arctic DMS flux (Chang et al., 2011). Indeed, observations
54 confirm that DMS oxidation products promote the growth of particles to produce aerosols
55 that may influence cloud processes and atmospheric albedo (Bigg and Leck, 2001; Rempillo
56 et al., 2011; Korhonen et al., 2008b; Chang et al., 2011). Arctic new particle formation
57 events and peaks in aerosol optical depth (AOD) occur during summertime clean air periods
58 (when levels of anthropogenic black carbon diminish), and have been linked to chlorophyll *a*
59 maxima in surface waters and the presence of aerosols formed from DMS oxidation products
60 such as methanesulfonate (MSA). The atmospheric oxidation products of DMS - SO₂ and
61 H₂SO₄ - contribute to both the growth of existing particles and new particle formation (NPF)
62 in the Arctic atmosphere (Leaitch et al., 2013; Gabric et al., 2014; Sharma et al., 2012). Thus,
63 the ongoing and projected rapid loss of seasonal Arctic sea ice may influence the Arctic
64 radiation budget via changes to both the DMS flux and the associated formation and growth
65 of cloud-influencing particles (Sharma et al., 2012). The influence that OA will have on the
66 production and flux of DMS, and how this may further influence the Arctic radiative balance,
67 is poorly understood and requires further experimental and modelling efforts.

68 During its short but highly productive summer season, the Southern Ocean is a hotspot of
69 DMS flux to the atmosphere, influenced by the prevalence of intense blooms of DMSP-rich
70 *Phaeocystis antarctica* (Schoemann et al., 2005) and the presence of persistent high winds
71 particularly in regions north of the sub-Antarctic front (Jarníková and Tortell, 2016). Around
72 3.4 Tg of sulfur is released from the Southern Ocean to the atmosphere between December
73 and February, a flux that represents ~15 % of global annual emissions of DMS (Jarníková
74 and Tortell, 2016). Elevated CCN numbers are seen in the most biologically active regions of
75 the Southern Ocean, with a significant contribution from DMS-driven secondary aerosol

76 formation processes (McCoy et al., 2015; Korhonen et al., 2008a). DMS-derived aerosols
77 from this region are estimated to contribute 6 to 10 $W m^{-2}$ to reflected short wavelength
78 radiation, similar to the influence of anthropogenic aerosols in the polluted Northern
79 Hemisphere (McCoy et al., 2015). Given this important influence of polar DMS emissions on
80 atmospheric processes and climate, it is vital we increase our understanding of the influence
81 of future ocean acidification on DMS production.

82 The polar oceans are characterised by high dissolved inorganic carbon (C_T) concentrations
83 and a low carbonate system buffering capacity, mainly due to the increased solubility of CO_2
84 in cold waters (Sabine et al., 2004; Orr et al., 2005). This makes these regions particularly
85 susceptible to the impacts of ocean acidification (OA). For example, extensive carbonate
86 mineral undersaturation is expected to occur in Arctic waters within the next 20 – 80 years
87 (McNeil and Matear, 2008; Steinacher et al., 2009). OA has already led to a 0.1 unit decrease
88 in global surface ocean pH, with a further fall of ~ 0.4 units expected by the end of the century
89 (Orr et al., 2005). The greatest declines in pH are likely in the Arctic Ocean with a predicted
90 fall of 0.45 units by 2100 (Steinacher et al., 2009), with a fall of ~ 0.3 units predicted for the
91 Southern Ocean (McNeil and Matear, 2008; Hauri et al., 2016). OA is occurring at a rate not
92 seen on Earth for 300 Ma, and so the potential effects on marine organisms, communities and
93 ecosystems could be wide-ranging and severe (Raven et al., 2005; Hönisch et al., 2012).

94 Despite the imminent threat to polar ecosystems and the importance of DMS emissions to
95 atmospheric processes, our knowledge of the response of polar DMS production to OA is
96 limited to a single mesocosm experiment performed in a coastal fjord in Svalbard (Riebesell
97 et al., 2013a; Archer et al., 2013) and one shipboard microcosm experiment with seawater
98 collected from Baffin Bay (Hussherr et al., 2017). Both studies reported significant
99 reductions in DMS concentrations with increasing levels of pCO_2 during seasonal
100 phytoplankton blooms. Hussherr et al. (2017) also saw reductions in total DMSP whilst

101 Archer et al. (2013) observed a significant increase in this compound, driven by CO₂-induced
102 increases in growth and abundance of dinoflagellates. However, these two single studies
103 provide limited information on the wider response of the open Arctic or Southern Oceans.

104 Mesocosm experiments have been a critical tool for assessing OA effects on surface ocean
105 communities (Engel et al., 2005; Engel et al., 2008; Schulz et al., 2008; Hopkins et al., 2010;
106 Schulz et al., 2013; Webb et al., 2015; Kim et al., 2006; Kim et al., 2010; Crawford et al.,
107 2016; Webb et al., 2016). The response of DMS to OA has been examined several times,
108 predominantly at the same site in Norwegian coastal waters (Vogt et al., 2008; Hopkins et al.,
109 2010; Webb et al., 2015; Avgoustidi et al., 2012), twice in Korean coastal waters (Kim et al.,
110 2010; Park et al., 2014), and a single study in the coastal Arctic waters of Svalbard (Archer et
111 al., 2013). Mesocosm enclosures, ranging in volume from ~11,000 – 50,000 L, allow the
112 response of surface ocean communities to a range of CO₂ treatments to be monitored under
113 near-natural light and temperature conditions over time scales (weeks - months). This is
114 sufficient time to allow a ‘winners vs loser’ dynamic to develop, whereby the succession of
115 the phytoplankton community is altered due to the differing sensitivities of different
116 taxonomic groups to changes in carbonate chemistry (Bach et al., 2017). The response of
117 DMS cycling to elevated CO₂ is generally driven by changes to the microbial community
118 structure (Brussaard et al., 2013; Archer et al., 2013; Hopkins et al., 2010; Engel et al., 2008).

119 The pseudo-natural conditions of mesocosm experiments offer the benefit of the inclusion of
120 community dynamics of three or more trophic levels, providing the opportunity to investigate
121 the influence of ecosystem dynamics on biogeochemical processes under experimental
122 conditions (Riebesell et al., 2013b). Furthermore, physical processes such as particle export
123 (Bach et al., 2016), which would be excluded by smaller scale experiments, can be
124 considered within the holistic mesocosm framework, and make the results relevant for use
125 within Earth system models (Six et al. 2013). However, the size, construction and associated

126 costs of mesocosms has limited their deployment to coastal/sheltered waters, resulting in
127 minimal geographical coverage, and leaving large gaps in our understanding of the response
128 of open ocean phytoplankton communities to OA.

129 Here, we adopt an alternative but complementary approach to explore the effects of OA on
130 the cycling of DMS with the use of short-term shipboard microcosm experiments. We build
131 on the previous temperate NW European shelf studies of Hopkins & Archer (2014) by
132 presenting data from four previously unpublished experiments from the NW European shelf
133 cruise, and by extending our experimental approach to the Arctic and Southern Oceans.

134 Vessel-based research enables multiple short term (days) near-identical incubations to be
135 performed over extensive spatial scales, that encompass natural gradients in carbonate
136 chemistry, temperature and nutrients (Richier et al., 2014; Richier et al., 2018). This allows
137 an assessment to be made of how a range of surface ocean communities, adapted to a variety
138 of environmental conditions, respond to the same driver. The focus is then on the effect of
139 short-term CO₂ exposure on physiological processes, as well as the extent of the variability in
140 acclimation between communities. The capacity of organisms to acclimate to changing
141 environmental conditions contributes to the resilience of key ecosystem functions, such as
142 DMS production. Therefore, do spatially-diverse communities respond differently to short
143 term OA, and can this be explained by the range of environmental conditions to which each is
144 presumably already adapted? The rapid CO₂ changes implemented in this study, and during
145 mesocosm studies, are far from representative of the predicted rate of change to seawater
146 chemistry over the coming decades, and the potential to induce a ‘shock’ response to the
147 sudden alteration of carbonate chemistry should be considered, particularly when working at
148 the smaller microcosm scale. Nevertheless, our approach can provide insight into the
149 physiological response and level of sensitivity to future OA of a variety of surface ocean

150 communities adapted to different in situ carbonate chemistry environments (Stillman and
151 Paganini, 2015), alongside the implications this may have for DMS production.

152 Communities of the NW European shelf consistently responded to acute OA with significant
153 increases in net DMS production, likely a result of an increase in stress-induced algal
154 processes (Hopkins and Archer, 2014). Do polar phytoplankton communities, which are
155 potentially adapted to contrasting biogeochemical environments, respond in the same way?
156 By expanding our approach to encompass both polar oceans, we can assess regional contrasts
157 in response. To this end, we combine our findings for temperate waters with those for the
158 polar oceans into a meta-analysis to advance our understanding of the regional variability and
159 drivers in the DMS response to OA.

160 **2 Material and Methods**

161 **2.1 Sampling stations**

162 This study presents new data from two sets of field experiments carried out as a part of the
163 UK Ocean Acidification Research Programme (UKOA) aboard the RRS James Clark Ross in
164 the sub-Arctic and Arctic in June-July 2012 (JR271) and in the Southern Ocean in January-
165 February 2013 (JR274). Data are combined with the results from an earlier study on board the
166 RRS Discovery (D366) described in Hopkins & Archer (2014) performed in the temperate
167 waters of the NW European shelf. Additionally, four previously unpublished experiments
168 from D366 are also included (E02b, E04b, E05b, E06) as well as two temperate experiments
169 from JR271 (NS and IB) (see Table 1). In total, 18 incubations were performed; 11 in
170 temperate and sub-Arctic waters of the NW European shelf and North Atlantic, 3 in Arctic
171 waters and 4 in the Southern Ocean. Figure 1 shows the cruise tracks, surface concentrations
172 of DMS and total DMSP (DMSPt) at CTD sampling stations as well as the locations of
173 sampling for shipboard microcosms (See Table 1 for further details).

174 **2.2 Shipboard microcosm experiments**

175 The general design and implementation of the experimental microcosms for JR271 and
176 JR274 was essentially the same as for D366 and described in Richier et al. (2014), (2018) and
177 Hopkins & Archer (2014), but with the additional adoption of trace metal clean sampling and
178 incubation techniques in the low trace metal open ocean waters (see Richier et al. (2018)). At
179 each station, pre-dawn vertical profiles of temperature, salinity, oxygen, fluorescence,
180 turbidity and irradiance were used to choose and characterise the depth of experimental water
181 collection. Subsequently, water was collected within the mixed layer from three successive
182 separate casts of a trace-metal clean titanium CTD rosette comprising twenty-four 10 L
183 Niskin bottles. Depth profiles of auxiliary measurements are shown in Figure 2. Each cast
184 was used to fill one of a triplicated set of experimental bottles (locations and sample depths,
185 Table 1). Bottles were sampled within a class-100 filtered air environment within a trace
186 metal clean container to avoid contamination during the set up. The water was directly
187 transferred into acid-cleaned 4.5 L polycarbonate bottles using acid-cleaned silicon tubing,
188 with no screening or filtration.

189 The carbonate chemistry within the experimental bottles was manipulated by addition of
190 equimolar HCl and NaHCO_3^- (1 mol L^{-1}) to achieve a range of CO_2 treatments: Mid CO_2
191 (Target: $550 \mu\text{atm}$), High CO_2 (Target: $750 \mu\text{atm}$), High+ CO_2 (Target: $1000 \mu\text{atm}$) and
192 High++ CO_2 (Target: $2000 \mu\text{atm}$) (Gattuso et al., 2010). Three treatment levels were used
193 during the sub-Arctic/Arctic microcosms (Mid, High, High+). For Southern Ocean
194 experiments, two experiments (*Drake Passage* and *Weddell Sea*) considered one CO_2
195 treatments (High). Three CO_2 treatments (High, High+, High++) were tested in the last two
196 experiments (*South Georgia* and *South Sandwich*). Full details of the carbonate chemistry
197 manipulations can be found in Richier et al. (2014) and Richier et al. (2018). Broadly,
198 achieved $p\text{CO}_2$ levels were well-matched to target values at the start of the experiments (0 h),

199 although differences in $p\text{CO}_2$ between target and initial values were greater in the higher
200 $p\text{CO}_2$ treatments, due to lowered carbonate system buffer capacity at higher $p\text{CO}_2$. For all 18
201 experiments, actual $p\text{CO}_2$ values at 0 h were on average around $89\% \pm 12\%$ (± 1 SD) of
202 target values. The attained $p\text{CO}_2$ values, and $p\text{CO}_2$ at each experimental time point, are
203 presented in Figures 3 and 4. After first ensuring the absence of bubbles or headspace, the
204 bottles were sealed with high density polyethylene (HDPE) lids with silicone/
205 polytetrafluoroethylene (PTFE) septa and placed in the incubation container. Bottles were
206 incubated inside a custom-designed temperature- and light-controlled shipping container, set
207 to match ($\pm < 1^\circ\text{C}$) the *in situ* water temperature at the time of water collection (shown in
208 Table 1) (see Richier et al. 2018). A constant light level ($100 \mu\text{E m}^{-2} \text{s}^{-1}$) was provided by
209 daylight simulating LED panels (Powerpax, UK). The light period within the microcosms
210 was representative of *in situ* conditions. For the sub-Arctic/Arctic Ocean stations,
211 experimental bottles were subjected to continuous light representative of the 24 h daylight of
212 the Arctic summer. For Southern Ocean and all temperate water stations, an 18:6 light: dark
213 cycle was used. Each bottle belonged to a set of triplicates, and sacrificial sampling of bottles
214 was performed at two time points (see Table 1 for exact times). Use of three sets of triplicates
215 for each time point allowed for the sample requirements of the entire scientific party (3 x 3
216 bottles, x 2 time points (see Table 1 for specific times for each experiment), x 4 CO_2
217 treatments = 72 bottles in total). Experiments were run for between 4 and 7 days (96 h – 168
218 h) (15 out of 18 experiments), with initial sampling proceeded by two further time points. For
219 three temperate experiments (E02b, E04b, E05b see Table 1 and Table 2) shorter two day
220 incubations were performed, with a single sampling point at the end. E06 was run for 96 h
221 (Table 1 and 2). Incubation times were extended for Southern Ocean stations *Weddell Sea*,
222 *South Georgia* and *South Sandwich* (see Table 1) as minimal CO_2 response, attributed to
223 slower microbial metabolism at low water temperatures, was observed for Arctic stations and

224 the first Southern Ocean station *Drake Passage*. The differential growth/metabolic rates
225 between temperate and polar waters justify the comparison of response of shorter duration
226 temperate experiments and longer duration polar experiments. The magnitude of response
227 was not related to incubation times, and expected differences in net growth rates (2- to 3-fold
228 higher in temperate compared to polar waters (Eppley, 1972)) did not account for the
229 differences in response magnitude despite the increased incubation time in polar waters (see
230 Richier et al. (2018) for detailed discussion). Samples for carbonate chemistry measurements
231 were taken first, followed by sampling for DMS, DMSP and related parameters.

232 **2.3 Standing stocks of DMS and DMSP**

233 Methods for the determination of seawater concentrations of DMS and DMSP are identical to
234 those described in Hopkins & Archer (2014) and will therefore be described in brief here.
235 Seawater DMS concentrations were determined by cryogenic purge and trap, with gas
236 chromatography and pulsed flame photometric detection (GC-PFPD) (Archer et al., 2013).
237 DMSP concentrations were measured as DMS following alkaline hydrolysis. Samples for
238 total DMSP concentrations from temperate waters were fixed by addition of 35 μ l of 50 %
239 H_2SO_4 to 7 mL of seawater (Kiene and Slezak, 2006), and analysed following hydrolysis
240 within 2 months of collection (Archer et al., 2013). Samples of DMSP that were collected in
241 polar waters were hydrolysed within 1 h of sample collection and analysed 6 – 12 h later. The
242 H_2SO_4 fixation method was not used for samples from polar waters given the likely
243 occurrence of *Phaeocystis sp.* which can result in the overestimation of DMSP concentrations
244 (del Valle et al., 2009). Similarly, concentrations of DMSPp were determined at each time
245 point by gravity filtering 7 ml of sample onto a 25 mm GF/F filter and preserving the filter in
246 7 ml of 35 mM H_2SO_4 in MQ-water (temperate samples) or immediately hydrolysing (polar
247 samples) and analysing by GC-PFPD. DMS calibrations were performed using alkaline cold-

248 hydrolysis (1 M NaOH) of DMSP sequentially diluted three times in MilliQ water to give
249 working standards in the range 0.03 – 3.3 ng S mL⁻¹. Five point calibrations were performed
250 every 2 – 4 days throughout the cruise.

251 **2.4 *De novo* DMSP synthesis**

252 *De novo* DMSP synthesis and gross production rates were determined for all microcosm
253 experiments, except *Barents Sea* and *South Sandwich*, at each experimental time point, using
254 methods based on the approach of Stefels et al. (2009) and described in detail in Archer et al.
255 (2013) and Hopkins and Archer (2014). Triplicate rate measurements were determined for
256 each CO₂ level. For each rate measurement three x 500 mL polycarbonate bottles were filled
257 by gently siphoning water from each replicate microcosm bottle. Trace amounts of
258 NaH¹³CO₃, equivalent to ~6 % of *in situ* dissolved inorganic carbon (*C_T*), were added to each
259 500 mL bottle. The bottles were incubated in the microcosm incubation container with
260 temperature and light levels as described earlier. Samples were taken at 0 h, then at two
261 further time points over a 6 - 9 h period. At each time point, 250 mL was gravity filtered in
262 the dark through a 47 mm GF/F filter, the filter gently folded and placed in a 20 mL serum
263 vial with 10 mL of Milli-Q and one NaOH pellet, and the vial was crimp-sealed. Samples
264 were stored at -20°C until analysis by proton transfer reaction-mass spectrometer (PTR-MS)
265 (Stefels et al. 2009).

266 The specific growth rate of DMSP (μ DMSP) was calculated assuming exponential growth
267 from:

$$268 \mu_t(\Delta t^{-1}) = \alpha_k \times \text{AVG} \left[\ln \left(\frac{{}^{64}\text{MP}_{\text{eq}} - {}^{64}\text{MP}_{t-1}}{{}^{64}\text{MP}_{\text{eq}} - {}^{64}\text{MP}_t} \right), \ln \left(\frac{{}^{64}\text{MP}_{\text{eq}} - {}^{64}\text{MP}_t}{{}^{64}\text{MP}_{\text{eq}} - {}^{64}\text{MP}_{t+1}} \right) \right] \quad 1$$

269 (Stefels et al. 2009) where ${}^{64}\text{MP}_t$, ${}^{64}\text{MP}_{t-1}$, ${}^{64}\text{MP}_{t+1}$ are the proportion of $1 \times {}^{13}\text{C}$ labelled
270 DMSP relative to total DMSP at time t , at the preceding time point ($t-1$) and at the subsequent
271 time point ($t+1$), respectively. Values of ${}^{64}\text{MP}$ were calculated from the protonated masses of
272 DMS as: $\text{mass } 64 / (\text{mass } 63 + \text{mass } 64 + \text{mass } 65)$, determined by PTR-MS. ${}^{64}\text{MP}_{\text{eq}}$ is the
273 theoretical equilibrium proportion of $1 \times {}^{13}\text{C}$ based on a binomial distribution and the
274 proportion of tracer addition. An isotope fractionation factor α_k of 1.06 is included, based on
275 laboratory culture experiments using *Emiliana huxleyi* (Stefels et al. 2009). In vivo DMSP
276 gross production rates during the incubations ($\text{nmol L}^{-1} \text{ h}^{-1}$) were calculated from μDMSP
277 and the initial particulate DMSP (DMSPp) concentration of the incubations (Hopkins &
278 Archer 2014, Stefels et al. 2009). These rates provide important information on how the
279 physiological status of DMSP-producing cells may be affected by OA within the bioassays.

280 **2.5 Seawater carbonate chemistry analysis**

281 The techniques and methods used to determine both the *in situ* and experimental carbonate
282 chemistry parameters, and to manipulate seawater carbonate chemistry within the
283 microcosms, are described in Richier et al. (2014) and will be only given in brief here.
284 Experimental T_0 measurements were taken directly from CTD bottles, and immediately
285 measured for total alkalinity (A_T) (Apollo SciTech AS-Alk2 Alkalinity Titrator) and
286 dissolved inorganic carbon (C_T) (Apollo SciTech C_T analyser (AS-C3) with LICOR 7000).
287 The CO2SYS programme (version 1.05) (Lewis and Wallace, 1998) was used to calculate the
288 remaining carbonate chemistry parameters including $p\text{CO}_2$.

289 Measurements of T_A and C_T were made from each bottle at each experimental time point and
290 again used to calculate the corresponding values for $p\text{CO}_2$ and pH_T . The carbonate chemistry
291 data for each sampling time point for each experiment are summarised in Supplementary
292 Table S1, S2 and S3 (Experimental starting conditions are given in Table 1).

293 **2.6 Chlorophyll a (Chl *a*) determinations**

294 Concentrations of Chl *a* were determined as described in Richier et al. (2014). Briefly, 100
295 mL aliquots of seawater from the incubation bottles were filtered through either 25 mm GF/F
296 (Whatman, 0.7 μm pore size) or polycarbonate filters (Whatman, 10 μm pore size) to yield
297 total and >10 μm size fractions, with the <10 μm fraction calculated by difference. Filters
298 were extracted in 6 mL HPLC-grade acetone (90%) overnight in a dark refrigerator.
299 Fluorescence was measured using a Turner Designs Trilogy fluorometer, which was regularly
300 calibrated with dilutions of pure Chl *a* (Sigma, UK) in acetone (90%).

301 **2.8 Community composition**

302 Small phytoplankton community composition was assessed by flow cytometry. For details of
303 methodology, see Richier et al. (2014).

304 **2.9 Data handling and statistical analyses**

305 Permutational analysis of variance (PERMANOVA) was used to analyse the difference in
306 response of DMS and DMSP concentrations to OA, both between and within the two polar
307 cruises in this study. Both dependant variables were analysed separately using a nested
308 factorial design with three factors; (i) Cruise Location: Arctic and Southern Ocean, (ii)
309 Experiment location nested within Cruise location (see Table 1 for station IDs) and (iii) CO₂
310 level: 385, 550, 750, 1000 and 2000 μatm . Main effects and pairwise comparisons of the
311 different factors were analysed through unrestricted permutations of raw data. If a low
312 number of permutations were generated then the *p*-value was obtained through random
313 sampling of the asymptotic permutation distribution, using Monte Carlo tests.

314 One-way analysis of variance was used to identify differences in ratio of >10 μm Chl *a* to
315 total Chl *a* ($\text{chl}_{>10\mu\text{m}} : \text{chl}_{\text{tot}}$, see Discussion). Initially, tests of normality were applied ($p < 0.05$)

316 = not normal), and if data failed to fit the assumptions of the test, linearity transformations of
317 the data were performed (logarithmic or square root), and the ANOVA proceeded from this
318 point. The results of ANOVA are given as follows: F = ratio of mean squares, df = degrees of
319 freedom, p = level of confidence. For those data still failing to display normality following
320 transformation, a rank-based Kruskal-Wallis test was applied (H = test statistic, df = degrees
321 of freedom, p = level of confidence).

322 **3 Results**

323 **3.1 Sampling stations**

324 At temperate sampling stations, sea surface temperatures ranged from 10.7°C for *Iceland*
325 *Basin*, to 15.3°C for *Bay of Biscay*, with surface salinity in the range 34.1 – 35.2, with the
326 exception of station E05b which had a relatively low salinity of 30.5 (Figure 2 and Table 1).
327 Seawater temperatures at the polar microcosm sampling stations ranged from -1.5°C at sea-
328 ice influenced stations (*Greenland Ice-edge* and *Weddell Sea*) up to 6.5°C for *Barents Sea*
329 (Fig. 2 A). Salinity values at all the Southern Ocean stations were <34, whilst they were ~35
330 at all the Arctic stations with the exception of *Greenland Ice-edge* which had the lowest
331 salinity of 32.5 (Fig. 2 B). Phototrophic nanoflagellate abundances were variable, with >3 x
332 10⁴ cells mL⁻¹ at *Greenland Gyre*, 1.5 x 10⁴ cells mL⁻¹ at *Barents Sea* and <3 x 10³ cells mL⁻¹
333 for all other stations (Fig. 2 D). Total bacterial abundances ranged from 3 x 10⁵ cells mL⁻¹ at
334 *Greenland Ice-edge* up to 3 x 10⁶ cells mL⁻¹ at *Barents Sea* (Fig. 2 E).

335 Chl *a* concentrations in temperate waters ranged from 0.3 µg L⁻¹ for two North Sea stations
336 (*E05* and *North Sea*) up to 3.5 µg L⁻¹ for *Irish Sea* (Figure 2 and Table 1). Chl *a* was also
337 variable in polar waters, exceeding 4 µg L⁻¹ at *South Sandwich* and 2 µg L⁻¹ at *Greenland Ice-*
338 *edge*, whilst the remaining stations ranged from 0.2 µg L⁻¹ (*Weddell Sea*) to 1.5 µg L⁻¹

339 (*Barents Sea*) (Figure 2). The high Chl *a* concentrations at *South Sandwich* correspond to low
340 in-water irradiance levels at this station (Fig. 2 C).

341 In temperate waters, maximum DMS concentrations were generally seen in near surface
342 measurements, ranging from 1.0 nmol L⁻¹ for *E04* to 21.1 nmol L⁻¹ for *E06*, with rapidly
343 decreasing concentrations with depth (Figure 2 G). As an exception to this, DMS
344 concentrations at *South Sandwich* showed a sub-surface maximum of 15 nM at 32 m,
345 coincident with a subsurface Chl *a* maximum of 5.4 µg L⁻¹. DMSP generally ranged from 12
346 – 20 nmol L⁻¹, except *Barents Sea* where surface concentrations exceeded 60 nmol L⁻¹
347 (Figure 2 H). DMSP tended to peak in the near surface waters, ranging from 12.0 nmol L⁻¹
348 for *E04* to 72.5 nmol L⁻¹ for *E06*, although in some cases a subsurface maximum in overall
349 DMSP concentrations was seen, as observed for *E05b* (89.8 nmol L⁻¹ 20 m), and again
350 coincident with a subsurface Chl *a* peak of >2 µg L⁻¹ (Figure 2 F and H). Surface DMS
351 concentrations in polar waters were generally lower than temperate waters, ranging from 1 –
352 3 nmol L⁻¹, with the exception of *South Sandwich* where concentrations of ~12 nmol L⁻¹ were
353 observed (Figure 2 G), and resulted in high DMS:DMSP of 0.6 – 0.9 in the surface layer
354 (Figure 2 I). DMS:DMSP did not exceed 0.5 at any other sampling stations.

355 **3.2 Response of DMS and DMSP to OA**

356 The temporal trend in DMS concentrations showed a similar pattern for the three Arctic
357 Ocean experiments. Initial concentrations of 1 – 2 nmol L⁻¹ remained relatively constant over
358 the first 48 h and then showed small increases of 1 - 4 nmol L⁻¹ over the remainder of the
359 incubation period (Figure 3). Increased variability between triplicate incubations became
360 apparent in all three Arctic experiments by 96 h, but no significant effects of elevated CO₂ on
361 DMS concentrations were observed. Initial DMSP concentrations were more variable, from 6
362 nmol L⁻¹ at *Greenland Ice-edge* to 12 nmol L⁻¹ at *Barents Sea*, and either decreased slightly

363 (net loss 1 – 2 nmol L⁻¹ GG), or increased slightly (net increase ~4 nmol L⁻¹ *Greenland Ice-*
364 *edge*, ~3 nmol L⁻¹ *Barents Sea*) (Figure 5 A – C). DMSP concentrations were found to
365 decrease significantly in response to elevated CO₂ after 48 h for *Barents Sea* (Fig. 5 C, $t =$
366 2.05, $p = 0.025$), whilst no significant differences were seen after 96 h. No other significant
367 responses in DMSP were identified.

368 The range of initial DMS concentrations was greater at Southern Ocean sampling stations
369 compared to the Arctic, from 1 nmol L⁻¹ at *Drake Passage* up to 13 nmol L⁻¹ at *South*
370 *Sandwich* (Figure 4). DMS concentrations showed little change over the course of 96 – 168 h
371 incubations and no effect of elevated CO₂, with the exception of *South Sandwich* (Fig. 4 D).
372 Here, concentrations decreased sharply after 96 h by between 3 and 11 nmol L⁻¹.
373 Concentrations at 96 h were CO₂-treatment dependent, with significant decreases in DMS
374 concentration occurring with increasing levels of CO₂ (PERMANOVA, $t = 2.61$, $p = 0.028$).
375 Significant differences ceased to be detectable by the end of the incubations (168 h). Initial
376 DMSP concentrations were higher at the Southern Ocean stations than for Arctic stations,
377 ranging from 13 nmol L⁻¹ for *Weddell Sea* to 40 nmol L⁻¹ for *South Sandwich* (Figure 5 D –
378 G). Net increases in DMSP occurred throughout, except at *South Georgia*, and were on the
379 order of between <10 nmol L⁻¹ - >30 nmol L⁻¹ over the course of the incubations.
380 Concentrations were not generally p CO₂-treatment dependent with the exception of the final
381 time point at *South Georgia* (144 h) when a significantly lower DMSP with increasing CO₂
382 was observed (PERMANOVA, $t = -5.685$, $p < 0.001$).

383 Results from the previously unpublished experiments from temperate waters are in strong
384 agreement with the five experiments presented in Hopkins and Archer (2014), with
385 consistently decreased DMS concentrations and enhanced DMSP under elevated CO₂. The
386 data is presented in the Supplementary Information, Table S4 and Figure S2, and included in
387 the meta-analysis in section 4.1 of this paper.

388 3.3 Response of de novo DMSP synthesis and production to OA

389 Rates of *de novo* DMSP synthesis (μDMSP) at initial time points ranged from 0.13 d^{-1}
390 (*Weddell Sea*, Fig. 6 G) to 0.23 d^{-1} (*Greenland Ice-edge*, Fig. 6 C), whilst DMSP production
391 ranged from $0.4 \text{ nmol L}^{-1} \text{ d}^{-1}$ (*Greenland Gyre*, Fig. 6 B) to $2.27 \text{ nmol L}^{-1} \text{ d}^{-1}$ (*Drake Passage*,
392 Fig. 6 F). Maximum rates of μDMSP of $0.37 - 0.38 \text{ d}^{-1}$ were observed at *Greenland Ice-edge*
393 after 48 h of incubation in all CO_2 treatments (Fig. 6 C). The highest rates of DMSP
394 production were observed at *South Georgia* after 96 h of incubation, and ranged from $4.1 -$
395 $6.9 \text{ nmol L}^{-1} \text{ d}^{-1}$ across CO_2 treatments (Fig. 6 J). Rates of DMSP synthesis and production
396 were generally lower than those measured in temperate waters (Hopkins and Archer, 2014)
397 (Initial rates: μDMSP $0.33 - 0.96 \text{ d}^{-1}$, $7.1 - 37.3 \text{ nmol L}^{-1} \text{ d}^{-1}$), but were comparable to
398 measurements made during an Arctic mesocosm experiment (Archer et al., 2013) ($0.1 - 0.25$
399 d^{-1} , $3 - 5 \text{ nmol L}^{-1} \text{ d}^{-1}$ in non-bloom conditions). The lower rates in cold polar waters likely
400 reflect slower metabolic processes and are reflected by standing stock DMSP concentrations
401 which were also lower than in temperate waters ($5 - 40 \text{ nmol L}^{-1}$ polar, $8 - 60 \text{ nmol L}^{-1}$
402 temperate (Hopkins and Archer, 2014)). No consistent effect of high CO_2 were observed for
403 either DMSP synthesis or production in polar waters, similar to findings for DMSP standing
404 stocks. However, some notable but contrasting differences between CO_2 treatments were
405 observed. There was a 36% and 37% increase in μDMSP and DMSP production respectively
406 at $750 \mu\text{atm}$ for the *Drake Passage* after 96 h (Figure 6 E, F), and a 38% and 44% decrease in
407 both at $750 \mu\text{atm}$ after 144 h for *Weddell Sea* (Figure 5 G, H). For *Drake Passage*, the
408 difference between treatments at 96 h coincided with significantly higher nitrate
409 concentrations in the High CO_2 treatment (Nitrate/nitrite at 96 h: Ambient = $18.9 \pm 0.2 \mu\text{mol}$
410 L^{-1} , $+\text{CO}_2 = 20.2 \pm 0.1 \mu\text{mol L}^{-1}$, ANOVA $F = 62.619$, $df = 1$, $p = 0.001$). However, it is
411 uncertain whether the difference in nutrient availability between treatments (approximately 5
412 %) would be significant enough to strongly influence the rate of DMSP production.

413 The differences in DMSP production rates did not correspond to any other measured
414 parameter. It is possible that changes in phytoplankton community composition may have led
415 to differences in DMSP production rates for *Drake Passage* and *Weddell Sea*, but no
416 quantification of large cells (diatoms, dinoflagellates) was undertaken for these experiments.

417 **4 Discussion**

418 **4.1 Regional differences in the response of DMS(P) to OA**

419 We combine our findings from the polar oceans with those from temperate waters into a
420 meta-analysis in order to assess the regional variability and drivers in the DMS(P) response to
421 OA. Figures 7 and 8 provide an overview of the results discussed so far in this current study,
422 together with the results from Hopkins & Archer (2014) as well as the results from 4
423 previously unpublished microcosm experiments from the NW European shelf cruise and a
424 further 2 temperate water microcosm experiments from the Arctic cruise (*North Sea* and
425 *Iceland Basin*, Table 1). This gives a total of 18 microcosm experiments, each with between 1
426 and 3 high CO₂ treatments.

427 Hopkins & Archer (2014) reported consistent and significant increases in DMS concentration
428 in response to elevated CO₂ that were accompanied by significant decreases in DMSPt
429 concentrations. Bacterially-mediated DMS processes appeared to be insensitive to OA, with
430 no detectable effects on dark rates of DMS consumption and gross production, and no
431 consistent response seen in bacterial abundance (Hopkins and Archer, 2014). In general,
432 there were large short-term decreases in Chl *a* concentrations and phototrophic nanoflagellate
433 abundance in response to elevated CO₂ in these experiments (Richier et al., 2014).

434 The relative treatment effects ($[x]_{\text{highCO}_2}/[x]_{\text{ambientCO}_2}$) for DMS and DMSP (Figure 7), DMSP
435 synthesis and production (Figure 8), and Chl *a* and phototrophic nanoflagellate abundance

436 (Figure 9) are plotted against the Revelle Factor of the sampled waters. The Revelle Factor
437 (R), calculated here with CO2Sys using measurements of carbonate chemistry parameters (R
438 $= (\Delta p\text{CO}_2/\Delta T\text{CO}_2)/(p\text{CO}_2/T\text{CO}_2)$, Lewis and Wallace, 1998), describes how the partial
439 pressure of CO_2 in seawater ($p\text{CO}_2$) changes for a given change in DIC (Sabine et al., 2004;
440 Revelle and Suess, 1957). Its magnitude varies latitudinally, with lower values (9 – 12) from
441 the tropics to temperate waters, and the highest values in cold high latitude waters (13 – 15).
442 Thus polar waters can be considered poorly buffered with respect to changes in DIC.
443 Therefore, biologically-driven seasonal changes in seawater $p\text{CO}_2$ would result in larger
444 changes in pH than would be experienced in temperate waters (Egleston et al., 2010).
445 Furthermore, the seasonal sea ice cycle strongly influences carbonate chemistry, such that sea
446 ice regions exhibit wide fluctuations in carbonate chemistry (Revelle and Suess, 1957; Sabine
447 et al., 2004). Sampling stations with a R above ~ 12 represent the seven polar stations (right of
448 red dashed line Fig. 7, 8, 9). The surface waters of the polar oceans have naturally higher
449 levels of DIC and a reduced buffering capacity, driven by higher CO_2 solubility in colder
450 waters (Sabine et al., 2004). Thus, the relationship between experimental response and R is a
451 simple way of demonstrating the differences in response to OA between temperate and polar
452 waters and provides some insight into how the CO_2 sensitivity of different surface ocean
453 communities may relate to the *in situ* carbonate chemistry. The effect of elevated CO_2 on
454 DMS concentrations at polar stations, relative to ambient controls, was minimal at both
455 sampling points, and is in strong contrast to the results from experiments performed in waters
456 with lower values of R on the NW European shelf. In contrast, at temperate stations, DMSP
457 concentrations displayed a clear negative treatment effect, whilst at polar stations a positive
458 effect was evident under high CO_2 and particularly at the first time point (48 – 96 h) (Fig. 7 C
459 and D). *De novo* DMSP synthesis and DMSP production rates show a less consistent
460 response in either environment (Fig. 8 A and B), although a significant suppression of

461 DMSP production rates in temperate waters compared to polar waters was seen (Fig. 8 B,
462 Kruskal-Wallis One Way ANOVA $H = 8.711$, $df = 1$, $p = 0.003$). A similar but not significant
463 response was seen for *de novo* DMSP synthesis (Fig. 8A).

464 Our data imply that DMSP concentrations in temperate waters were downregulated in
465 response to OA, attributed to the adverse effects of rapid OA on the growth of DMSP
466 producers which led to reductions in the abundance of these types of phytoplankton (Richier
467 et al. 2014, Hopkins and Archer 2014). By comparison, a more muted, but generally positive,
468 DMSP response was seen in polar waters at the first time point, whilst these treatment effects
469 were more or less undetectable by the second time point. There is some evidence that the
470 enhanced DMSP concentrations in polar waters were accompanied by increased DMSP
471 production rates (Figure 8), although data is not available for all experiments. However, these
472 changes may reflect a short term 'shock' physiological protective response to the
473 experimental OA, similar to that seen in response to other short term stressors such as high
474 irradiance that result in an increase in DMSP concentrations (Sunda et al., 2002; Galindo et
475 al., 2016). The lack of treatment effect in DMSP concentrations by the second time point may
476 be indicative that the community had, to some extent, acclimated to the change, allowing
477 DMSP production/concentrations to return to baseline levels. This may reflect a higher
478 degree of tolerance to rapid changes in carbonate chemistry amongst polar communities -
479 species which are already adapted to highly variable irradiance/carbonate chemistry regimes
480 (Thomas and Dieckmann, 2002; Rysgaard et al., 2012; Thøisen et al., 2015). Further
481 experiments with polar communities would help to unravel the potential importance of such
482 mechanisms and whether they facilitated the ability of polar phytoplankton communities to
483 resist the high CO₂ treatments.

484 The responses to OA observed for DMS and DMSP production are likely to be reflected in
485 the dynamics of the DMSP-producing phytoplankton. In an assessment across all

486 experiments, Richier et al. (2018) showed that the magnitude of biological responses to short
487 term CO₂ changes reflected the buffer capacity of the sampled waters. A consistent
488 suppression of net growth rates in small phytoplankton (<10 µm) and total Chl *a*
489 concentrations was observed under high CO₂ within experiments performed in temperate
490 waters with higher buffer capacity.

491 Generally, less significant relationships were found between the phytoplankton response and
492 the other wide range of physical, chemical or biological variables that were examined
493 (Richier et al. 2018).

494 In correspondence with the analyses carried out by Richier et al (2018), at 48 – 96 h (see
495 Table 1), a statistically significant difference in response was seen between temperate and
496 polar waters for Chl *a* (Kruskal-Wallis One Way ANOVA $H = 20.577$, $df = 1$, $p < 0.001$). In
497 general, at polar stations phytoplankton showed minimal response to elevated CO₂, in
498 contrast to a strong negative response in temperate waters (Fig. 9A). By the second time point
499 (96 – 144 h, see Table 1), no significant difference in response of Chl *a* between temperate
500 and polar waters was apparent (Fig. 9B). As shown in Richier et al. (2014), phototrophic
501 nanoflagellates responded to high CO₂ with large decreases in abundance in temperate waters
502 and increases in abundance in polar waters (Fig. 9 C and D), with some exceptions: *North*
503 *Sea* and *South Sandwich* gave the opposite response. The responses had lessened by the
504 second time point (96 – 168 h, see Table 1).

505 In contrast, bacterial abundance did not show the same regional differences in response to
506 high CO₂ (see Hopkins and Archer (2014) for temperate waters, and Figure S1,
507 supplementary information, for polar waters). Bacterial abundance in temperate waters gave
508 variable and inconsistent responses to high CO₂. For all Arctic stations, as well as Southern
509 Ocean stations *Drake Passage* and *Weddell Sea*, no response to high CO₂ was observed. For
510 *South Georgia* and *South Sandwich*, bacterial abundance increased at 1000 and 2000 µatm,

511 with significant increases for *South Georgia* after 144 h of incubation (ANOVA $F = 137.936$,
512 $p < 0.001$). Additionally, at Arctic stations *Greenland Gyre* and *Greenland Ice-edge*, no
513 overall effect of increased CO_2 on rates of DOC release, total carbon fixation or POC : DOC
514 was observed (Poulton et al. 2016).

515 Overall, the observed differences in the regional response of DMSP and DMS to carbonate
516 chemistry manipulation could not be attributed to any other measured factor that varied
517 systematically between temperate and polar waters. These include ambient nutrient
518 concentrations, which varied considerably but where direct manipulation had no influence on
519 the response, and initial community structure, which was not a significant predictor of the
520 phytoplankton response (Richier et al. 2018).

521 **4.2 Influence of community cell-size composition on DMS response**

522 It has been proposed that variability in the concentrations of carbonate species (e.g. $p\text{CO}_2$,
523 HCO_3^- , CO_3^{2-}) experienced by phytoplankton is related to cell size, such that smaller-celled
524 taxa ($< 10 \mu\text{m}$) with a reduced diffusive boundary layer are naturally exposed to relatively less
525 variability compared to larger cells (Flynn et al., 2012). Thus, short-term and rapid changes in
526 carbonate chemistry, such as the kind imposed during our microcosm experiments, may have
527 a disproportionate effect on the physiology and growth of smaller celled species. Larger cells
528 may be better able to cope with variability as normal cellular metabolism results in significant
529 cell surface changes in carbonate chemistry parameters (Richier et al., 2014). Indeed, the
530 marked response in DMS concentrations to short term OA in temperate waters has been
531 attributed to this enhanced sensitivity of small phytoplankton (Hopkins and Archer, 2014).
532 Was the lack of DMS response to OA in polar waters therefore a result of the target
533 communities being dominated by larger-celled, less carbonate-sensitive species?

534 Size-fractionated Chl *a* measurements give an indication of the relative contribution of large
535 and small phytoplankton cells to the community. For experiments in temperate waters, the
536 mean ratio of >10 μm Chl *a* to total Chl *a* (hereafter >10 μm : *total*) of 0.32 ± 0.08 was lower
537 than the ratio for polar stations of 0.54 ± 0.13 (Table 2). Although the difference was not
538 statistically significant, this might imply a tendency towards communities dominated by
539 larger cells in the polar oceans, which may partially explain the apparent lack of DMS
540 response to elevated CO_2 . However, this is not a consistent explanation for the observed
541 responses. For example, the Arctic *Barents Sea* station had the lowest observed >10 μm :
542 *total* of 0.04 ± 0.01 , suggesting a community comprised almost entirely of <10 μm cells; yet
543 the response to short term OA differed to the response seen in temperate waters. No
544 significant CO_2 effects on DMS or DMSP concentrations or production rates were observed
545 at this station, whilst total Chl *a* significantly increased under the highest CO_2 treatments
546 after 96 h (PERMANOVA $F = 33.239$, $p < 0.001$). Thus, our cell size theory does not hold for
547 all polar waters, suggesting that regardless of the dominant cell size, polar communities are
548 more resilient to OA. In the following section, we explore the causes of this apparent
549 insensitivity to OA in terms of the environmental conditions to which the communities have
550 presumably adapted.

551 **4.3 Adaptation to a variable carbonate chemistry environment**

552 Given that DMS production by polar phytoplankton communities appeared to be insensitive
553 to experimental OA compared to significant sensitivity in temperate communities, we
554 hypothesise that polar communities are adapted to greater natural variability in carbonate
555 chemistry over spatial and seasonal scales. This greater variability is partly the result of the
556 lower buffering capacity (Revelle Factor) of polar waters compared to lower latitude waters,
557 and partly due to specific processes that occur in the polar regions that strongly alter DIC

558 concentrations (e.g. sea ice formation and melt, enhanced CO₂ dissolution into cold polar
559 waters, upwelling of CO₂ rich water). Therefore, polar plankton communities are not only
560 subject to geophysical processes that strongly alter in situ carbonate chemistry on both spatial
561 and seasonal scales, but such changes are accompanied by larger pH changes than would
562 occur in more strongly buffered temperate waters. Therefore, polar surface ocean
563 communities are perhaps more likely to experience fluctuations between high pH and low pH
564 over relatively smaller time/space scales (Tynan et al., 2016). Thus below, we discuss our
565 findings in the context of the spatial pH variability we observed for each cruise track, and
566 explore some of the processes that drive this variability in polar waters. Information on the
567 pH variability at each sampling station is not available, so we cannot be certain of the exact
568 carbonate chemistry variability to which each of the sampled communities may have been
569 exposed and adapted. However, we can consider the overall variability in carbonate
570 chemistry over the spatial scales of the cruise tracks to demonstrate the characteristics of each
571 study area.

572 The polar waters sampled during our study were characterised by pronounced gradients in
573 carbonate chemistry over relatively small spatial scales. In underway samples taken along
574 each cruise track (Arctic Ocean 3500 nm, Southern Ocean 4000 nm), pH varied by 0.45 units
575 (8.00 – 8.45) in the Arctic, and 0.40 units (8.30 - 7.90) in the Southern Ocean (Tynan et al.
576 2016). In some cases this range in variability was seen over relatively small distances: Figure
577 4 in Tynan et al. (2016) shows that pH fluctuated from 8.45 and 8.0 over a distance of 50 –
578 100 miles in the sea-ice influenced Fram Strait. By comparison, pH varied by a total of 0.2
579 units (8.22 - 8.02) in underway samples from the NW European shelf sea cruise (Rerolle et
580 al. 2014). The observed horizontal gradients in polar waters were driven by different
581 physical and biogeochemical processes in each ocean. In the Arctic Ocean, this variability in
582 carbonate chemistry was partly driven by physical processes that controlled water mass

583 composition, temperate and salinity, particularly in areas such as the Fram Strait and
584 Greenland Sea. Along the ice-edge and into the Barents Sea, biological processes exerted a
585 strong control, as abundant iron resulted in high chlorophyll concentrations, low DIC and
586 elevated pH. By contrast, variations in temperature and salinity had only a small influence on
587 carbonate chemistry in the Southern Ocean in areas with iron limitation, and larger changes
588 were driven by a combination of calcification, advection and upwelling. Where iron was
589 replete, e.g. near South Georgia, biological DIC drawdown had a large impact on carbonate
590 chemistry (Tynan et al. 2016). A further set of processes was in play in sea ice influenced
591 regions. At the Arctic ice edge, abundant iron drove strong bloom development along the ice
592 edge, whilst sea ice retreat in the Southern Ocean was not always accompanied by iron
593 release (Tynan et al. 2016).

594 For comparison with Arctic stations, Hagens and Middelburg (2016) report a seasonal pH
595 variability of up to 0.25 units from a single site in the open ocean surface waters in the
596 Iceland Sea, whilst Kapsenberg et al. (2015) report an annual variability of 0.3 – 0.4 units in
597 the McMurdo Sound, Antarctica. This implies that both open ocean and sea ice-influenced
598 polar waters experience large variations in carbonate chemistry over seasonal cycles. By
599 contrast, monthly averaged surface $p\text{CO}_2$ data collected from station L4 in the Western
600 English Channel over the period 2007 – 2011 provides an example of typical carbonate
601 chemistry dynamics in NW European shelf sea waters. Over this period, pH had an annual
602 range of 0.15 units (8.05 – 8.20), accompanied by a range in $p\text{CO}_2$ of 302 – 412 μatm (Kitidis
603 et al., 2012).

604 The sea ice environment in particular is characterised by strong spatial and seasonal
605 variability in carbonate chemistry. Sea ice is inhabited by a specialised microbial community
606 with a complex set of metabolic and physiological adaptations allowing these organisms to
607 withstand wide fluctuations in pH up to as high as 9.9 in brine channels to as low as 7.5 in the

608 under-ice water (Thomas and Dieckmann, 2002; Rysgaard et al., 2012; Thoisen et al., 2015).
609 The open waters associated with the ice edge also experience strong gradients in pH and
610 other carbonate chemistry parameters. This can be attributed to two processes: 1. The strong
611 seasonal drawdown of DIC due to rapid biological uptake by phytoplankton blooms at the
612 productive ice edge which drives up pH. On the Arctic cruise, increases of up to 0.33 pH
613 units were attributed to such processes in this region (Tynan et al., 2016). The effect was less
614 dramatic in the Fe-limited and less productive Weddell Sea with gradients in pH ranging
615 from 8.20 – 8.10 (Tynan et al., 2016). 2. The drawdown of DIC is countered by the release
616 and accumulation of respired DIC under sea ice due to the degradation of organic matter.
617 However, this accumulation occurs in subsurface/bottom waters, which are isolated from the
618 productive surface mixed layer by strong physical stratification and hence, of less relevance
619 to the current study.

620 The influence of sea ice on carbonate chemistry combined with the strong biological
621 drawdown of DIC in polar waters may have influenced the ability of some of the
622 communities we sampled during our study to withstand the short term changes to carbonate
623 chemistry they experienced within the bioassays. Two of our sampling stations were ‘sea-ice
624 influenced’: *Greenland Ice Edge* and *Weddell Sea*. Both were in a state of sea ice retreat as
625 our sampling occurred in the summer months. Sampling for the *Greenland Ice Edge* station
626 was performed in open, deep water, near to an area of thick sea ice, with low fluorescence but
627 reasonable numbers of diatoms (Leakey, 2012). Similarly, the *Weddell Sea* station was
628 located near the edge of thick pack ice but in an area of open water that allowed sampling to
629 occur without hindrance by brash ice (Tarling, 2013). At both stations we saw little or no
630 response in DMS or DMSP to experimental acidification, which may imply that the *in situ*
631 communities were more or less adapted to fluctuations in pH. Our experimental OA resulted
632 in pH decreases of between 0.4 and 0.7 units. However, it is unclear whether the communities

633 we sampled were able to withstand the artificial pH perturbation because they were adapted
634 to living in sea ice, or whether they had adapted to cope with other fluctuations in carbonate
635 chemistry that occur in polar waters.

636 In summary, this demonstrates the high variability in carbonate chemistry, including pH,
637 which polar communities may experience relative to their temperate counterparts, and which
638 is partly driven by the lowered buffer capacity of polar waters to changes in DIC, relative to
639 the more well-buffered temperate waters. This may have resulted in polar communities that
640 have adapted to and are more resilient to experimentally-induced OA. Of course, it is
641 important to recognise that this data represent only a snapshot (4 – 6 weeks) of a year, and
642 thus does not contain information on the range in variability over daily and seasonal cycles,
643 timescales which might be considered most important in terms of the carbonate system
644 variability experienced by the cells and how this drives CO₂ sensitivity (Flynn et al. 2012;
645 Richier et al. 2018). Nevertheless, this inherent carbonate chemistry variability experienced
646 by organisms living in polar waters may equip them with the resilience to cope with both
647 experimental and future OA.

648 Adaptation to such natural variability may induce the ability to resist abrupt changes within
649 the polar biological community (Kapsenberg et al., 2015). This is manifested here as
650 negligible impacts on rates of *de novo* DMSP synthesis and net DMS production in the
651 microbial communities of the polar open oceans to short term changes in carbonate
652 chemistry. A number of previous studies in polar waters have reported similar findings.

653 Phytoplankton communities were able to tolerate a $p\text{CO}_2$ range of 84 – 643 μatm in ~12 d
654 minicosm experiments (650 L) in Antarctic coastal waters, with no effects on
655 nanophytoplankton abundance, and enhanced abundance of picophytoplankton and
656 prokaryotes (Davidson et al., 2016; Thomson et al., 2016). In experiments under the Arctic
657 ice, microbial communities demonstrated the capacity to respond either by selection or

658 physiological plasticity to elevated CO₂ during short term experiments (Monier et al., 2014).
659 Subarctic phytoplankton populations demonstrated a high level of resilience to OA in short
660 term experiments, suggesting a high level of physiological plasticity that was attributed to the
661 prevailing strong gradients in pCO₂ levels experienced in the sample region (Hoppe et al.,
662 2017). Furthermore, a more recent study describing ten CO₂ manipulation experiments in
663 Arctic waters found that primary production was largely insensitive to OA over a large range
664 of light and temperature levels (Hoppe et al., 2018). This supports our hypothesis that,
665 relative to temperate communities, polar microbial communities may have a high capacity to
666 compensate for environmental variability (Hoppe et al., 2018), and are thus already adapted
667 to, and are able to tolerate, large variations in carbonate chemistry. Thus by performing
668 multiple, replicated experiments over a broad geographic range, the findings of this study
669 imply that the DMS response may be both a reflection of: (i) the level of sensitivity of the
670 community to changes in the mean state of carbonate chemistry, and (ii) the regional
671 variability in carbonate chemistry experienced by different communities. This highlights the
672 limitations associated with simple extrapolation of results from a small number of
673 geographically-limited experiments e.g. Six et al. (2013). Such an approach lacks a
674 mechanistic understanding that would allow a model to capture the regional variability in
675 response that is apparent from the microcosms experiments presented here.

676 **4.4 Comparison to an Arctic mesocosm experiment**

677 Experimental data clearly provide useful information on the potential future DMS response to
678 OA, but these data become most powerful when incorporated in Earth System Models (ESM)
679 to facilitate predictions of future climate. To date, two modelling studies have used ESM to
680 assess the potential climate feedback resulting from the DMS sensitivity to OA (Six et al.,
681 2013;Schwinger et al., 2017), and both have used results from mesocosm experiments.
682 However, the DMS responses to OA within our short term microcosm experiments contrast

683 with the results of most previous mesocosm experiments, and of particular relevance to this
684 study, an earlier Arctic mesocosm experiment (Archer et al., 2013). Whilst no response in
685 DMS concentrations to OA was generally seen in the polar microcosm experiments discussed
686 here, a significant decrease in DMS with increasing levels of CO₂ in the earlier mesocosm
687 study was seen. Therefore, it is useful to consider how the differences in experimental design,
688 and other factors, between microcosms and mesocosms may result in contrasting DMS
689 responses to OA.

690 The short duration of the microcosm experiments (4 – 7 d) allows the physiological
691 (phenotypic) capacity of the community to changes in carbonate chemistry to be assessed. In
692 other words, how well is the community adapted to variable carbonate chemistry and how
693 does this influence its ability to acclimate to change? Although the mesocosm experiment
694 considered a longer time period (4 weeks), the first few days can be compared to the
695 microcosms. No differences in DMS or DMSP concentrations were detected for the first
696 week of the mesocosm experiment, implying a certain level of insensitivity of DMS
697 production to the rapid changes in carbonate chemistry. In fact, when taking all previous
698 mesocosm experiments into consideration, differences in DMS concentrations have
699 consistently been undetectable during the first 5 – 10 days, implying there is a limited short-
700 term physiological response by the in situ communities (Hopkins et al., 2010; Avgoustidi et
701 al., 2012; Vogt et al., 2008; Kim et al., 2010; Park et al., 2014). This is in contrast to the
702 strong response in the temperate microcosms from the NW European shelf (Hopkins and
703 Archer, 2014). However, all earlier mesocosm experiments have been performed in coastal
704 waters, which like polar waters, can experience a large natural range in carbonate chemistry.
705 In the case of coastal waters this is driven to a large extent by the influence of riverine
706 discharge and biological activity (Fassbender et al., 2016). Thus coastal communities may

707 also possess a higher level of adaptation to variable carbonate chemistry compared to the
708 open ocean communities of the temperate microcosms (Fassbender et al., 2016).

709 The later stages of mesocosm experiments address a different set of hypotheses, and are less
710 comparable to the microcosms reported here. With time, an increase in number of generations
711 leads to community structure changes and taxonomic shifts, driven by selection on the
712 standing genetic variation in response to the altered conditions. Moreover, the coastal Arctic
713 mesocosms were enriched with nutrients after 10 days, affording relief from nutrient
714 limitation and allowing differences between $p\text{CO}_2$ treatments to be exposed, including a
715 strong DMS(P) response.(Archer et al., 2013; Schulz et al., 2013). During this period of
716 increased growth and productivity, CO_2 increases drove changes which reflected both the
717 physiological and genetic potential within the community, and resulted in taxonomic shifts.
718 The resultant population structure was changed, with an increase in abundance of
719 dinoflagellates, particularly *Heterocapsa rotundata*. Increases in DMSP concentrations and
720 DMSP synthesis rates were attributed to the population shift towards dinoflagellates. The
721 drivers of the reduced DMS concentrations were less clear, but may have been linked to
722 reduced DMSP-lyase capacity within the dominant phytoplankton, a reduction in bacterial
723 DMSP lysis, or an increase in bacterial DMS consumption rates (Archer et al., 2013). Again,
724 this is comparable to all other mesocosm experiments, wherein changes to DMS
725 concentrations can be associated with CO_2 -driven shifts in community structure (Hopkins et
726 al., 2010; Avgoustidi et al., 2012; Vogt et al., 2008; Kim et al., 2010; Park et al., 2014; Webb
727 et al., 2015). However, given the lack of further experiments of a similar location, design and
728 duration to the Arctic mesocosm, it is unclear how representative the mesocosm result is of
729 the general community-driven response to OA in high latitude waters.

730 We did not generally see any broad-scale CO_2 -effects on community structure in polar
731 waters. This can be demonstrated by a lack of significant differences in the mean ratio of >10

732 μm Chl *a* to total Chl *a* ($>10 \mu\text{m} : \text{total}$) between CO_2 treatments, implying there were no
733 broad changes in community composition (Table 2). *South Sandwich* was an exception to
734 this, where large and significant increases in the mean ratio of $>10 \mu\text{m} : \text{total}$ were observed
735 at 750 μatm and 2000 μatm CO_2 relative to ambient CO_2 (ANOVA, $F = 207.144$, $p < 0.001$, df
736 $= 3$), demonstrating that even at the short timescale of the microcosm experiments it is
737 possible for some changes to community composition to occur. Interestingly, this was also
738 the only polar station that exhibited any significant effects on DMS after 96 h of incubation
739 (Figure 4 D). However, given the lack of similar response at 1000 μatm , it remains equivocal
740 whether this was driven by a CO_2 -effect or some other factor.

741 In contrast to our findings, a recent single 9 day microcosm experiment (Hussherr et al.,
742 2017) performed in Baffin Bay (Canadian Arctic) saw a linear 80% decrease in DMS
743 concentrations during spring bloom-like conditions. It should be noted that this response was
744 seen over a range of $p\text{CO}_2$ from 500 - 3000 μatm , far beyond the levels used in the present
745 study. Nevertheless, this implies that polar DMS production may be sensitive to OA at certain
746 times of the year, such as during the highly productive spring bloom, but less sensitive during
747 periods of low and stable productivity, such as the summer months sampled during this study.
748 Furthermore, a number of other studies from both the Arctic e.g. (Coello-Camba et al., 2014;
749 Holding et al., 2015; Thoisen et al., 2015) and the Southern Ocean e.g. (Trimborn et al.,
750 2017; Tortell et al., 2008; Hoppe et al., 2013) suggest that polar phytoplankton communities
751 can demonstrate sensitivity to OA, in contrast to our findings. This emphasises the need to
752 gain a more detailed understanding of both the spatial and seasonal variability in the polar
753 phytoplankton community and associated DMS response to changing ocean acidity.

754 **5 Conclusions**

755 We have shown that net DMS production by summertime polar open ocean microbial
756 communities is insensitive to OA during multiple, highly replicated short term microcosm
757 experiments. We provide evidence that, in contrast to temperate communities (Hopkins and
758 Archer, 2014), the polar communities we sampled were relatively insensitive to variations in
759 carbonate chemistry (Richier et al., 2018), manifested here as a minimal effect on net DMS
760 production. Our findings contrast with two previous studies performed in Arctic waters
761 (Archer et al. 2013; Hussherr et al. 2017) which showed significant decreases in DMS in
762 response to OA. These discrepancies may be driven by differences in experimental design,
763 variable sensitivity of microbial communities to changing carbonate chemistry between
764 different areas, or by variability in the response to OA depending on the time of year, nutrient
765 availability, and ambient levels of growth and productivity. This serves to highlight the
766 complex spatial and temporal variability in DMS response to OA which warrants further
767 investigation to improve model predictions.

768 Our results imply that the phytoplankton communities of the temperate microcosms initially
769 responded to the rapid increase in $p\text{CO}_2$ via a stress-induced response, resulting in large and
770 significant increases in DMS concentrations occurring over the shortest timescales (2 days),
771 with a lessening of the treatment effect with an increase in incubation time (Hopkins and
772 Archer 2014). The dominance of short response timescales in well-buffered temperate waters
773 may also indicate rapid acclimation of the phytoplankton populations following the initial
774 stress response, which forced the small-sized phytoplankton beyond their range of
775 acclimative tolerance and lead to increased DMS (Richier et al. 2018, Hopkins and Archer
776 2014). This supports the hypothesis that populations from higher latitude, less well-buffered
777 waters, already possess a certain degree of acclimative tolerance to variations in carbonate
778 chemistry environment. Although initial community size structure was not a significant
779 predictor of the response to high CO_2 , it is possible that a combination of both community

780 composition and the natural range in variability in carbonate chemistry – as a function of
781 buffer capacity – may influence the DMS/P response to OA over a range of timescales
782 (Richier et al. 2018).

783 Our findings should be considered in the context of timescales of change (experimental vs
784 real world OA) and the potential of microbial communities to adapt to a gradually changing
785 environment. Microcosm experiments focus on the physiological response of microbial
786 communities to short term OA. Mesocosm experiments consider a timescale that allows the
787 response to be driven by community composition shifts, but are not long enough in duration
788 to incorporate an adaptive response. Neither approach is likely to accurately simulate the
789 response to the gradual changes in surface ocean pH that will occur over the next 50 – 100
790 years, nor the resulting changes in microbial community structure and distribution. However,
791 we hypothesise that the DMS response to OA should be considered not only in relation to
792 experimental perturbations to carbonate chemistry, but also in relation to the magnitude of
793 background variability in carbonate chemistry experienced by the DMS-producing organisms
794 and communities. Our findings suggest a strong link between the DMS response to OA and
795 background regional variability in the carbonate chemistry.

796 Models suggest the climate may be sensitive to changes in the spatial distribution of DMS
797 emissions over global scales (Woodhouse et al., 2013; Menzo et al., 2018). Such changes
798 could be driven by both physiological and adaptive responses to environmental change.

799 Accepting the limitations of experimental approaches, our findings suggest that net DMS
800 production from polar oceans may be resilient to OA in the context of its short term effects
801 on microbial communities. The oceans face a multitude of CO₂-driven changes in the coming
802 decades, including OA, warming, deoxygenation and loss of sea ice (Gattuso et al., 2015).

803 Our study addresses only one aspect of these future ocean stressors, but contributes to our

804 understanding of how DMS emissions from the polar oceans may alter, facilitating a better
805 understanding of Earth's future climate.

806 **Data availability**

807 All data has been deposited in and is accessible from the British Oceanographic Data Centre.

808 **Author contributions**

809 CMM, SR, FH, PDN and SDA designed the experiments. FH and JAS conducted the
810 measurements, FH and GLC analysed the data. FH prepared the paper with assistance and
811 contributions from all co-authors.

812 **Competing interests**

813 The authors declare that they have no conflict of interest.

814 **Financial support**

815 This work was funded under the UK Ocean Acidification thematic programme (UKOA) via
816 the UK Natural Environment Research Council (NERC) grants to PD Nightingale and SD
817 Archer (NE/H017259/1) and to T Tyrell, EP Achterberg and CM Moore (NE/H017348/1).

818 The UK Department for Environment, Food and Rural Affairs (Defra) and the UK
819 Department of Energy and Climate Change (DECC) also contributed to funding UKOA. The
820 National Science Foundation, United States, provided additional support to SD Archer ((NSF
821 OCE-1316133).

822 **Review statement**

823 This paper was edited by Gerhard Herdl and reviewed by three anonymous referees.

824 **Acknowledgements**

825 Our work and transit in the coastal waters of Greenland, Iceland and Svalbard was granted
826 thanks to permissions provided by the Danish, Icelandic and Norwegian diplomatic
827 authorities. We thank the captains and crew of the RRS Discovery (cruise D366) and RRS
828 James Clark Ross (cruises JR271 and JR274), and the technical staff of the National Marine
829 Facilities and the British Antarctic Survey. We are grateful to Mariana Ribas-Ribas and
830 Eithne Tynan for carbonate chemistry data, Elaine Mitchell and Clement Georges for flow
831 cytometry data, and Mariana Ribas-Ribas and Rob Thomas (BODC) for data management.

832 **References**

- 833 Archer, S. D., Kimmance, S. A., Stephens, J. A., Hopkins, F. E., Bellerby, R. G. J., Schulz,
834 K. G., Piontek, J., and Engel, A.: Contrasting responses of DMS and DMSP to ocean
835 acidification in Arctic waters, *Biogeosciences*, 10, 1893-1908, 10.5194/bg-10-1893-2013,
836 2013.
- 837
838 Avgoustidi, V., Nightingale, P. D., Joint, I. R., Steinke, M., Turner, S. M., Hopkins, F. E.,
839 and Liss, P. S.: Decreased marine dimethyl sulfide production under elevated CO₂ levels in
840 mesocosm and in vitro studies, *Environ. Chem.*, 9, 399-404, 2012.
- 841
842 Bach, L.T., Boxhammer, T., Larsen, A., Hildebrandt, N., Schulz, K.G. and Riebesell, U.:
843 Influence of plankton community structure on the sinking velocity of marine aggregates.
844 *Global Biogeochemical Cycles*, 30(8), pp.1145-1165, 2016.
- 845
846 Bach, L.T., Alvarez-Fernandez, S., Hornick, T., Stuhr, A. and Riebesell, U.: Simulated ocean
847 acidification reveals winners and losers in coastal phytoplankton. *PloS one*, 12 (11),
848 p.e0188198, 2017.
- 849 Bigg, E. K., and Leck, C.: Properties of the aerosol over the central Arctic Ocean, *Journal of*
850 *Geophysical Research: Atmospheres*, 106, 32101-32109, 2001.
- 851
852 Brussaard, C. P. D., Noordeloos, A. A. M., Witte, H., Collentour, M. C. J., Schulz, K.,
853 Ludwig, A., and Riebesell, U.: Arctic microbial community dynamics influenced by elevated
854 CO₂ levels, *Biogeosciences*, 10, 719-731, 10.5194/bg-10-719-2013, 2013.
- 855
856 Carpenter, L. J., Archer, S. D., and Beale, R.: Ocean-atmosphere trace gas exchange,
857 *Chemical Society Reviews*, 41, 6473-6506, 2012.
- 858
859 Chang, R. Y. W., Sjostedt, S. J., Pierce, J. R., Papakyriakou, T. N., Scarratt, M. G., Michaud,
860 S., Levasseur, M., Leitch, W. R., and Abbatt, J. P.: Relating atmospheric and oceanic DMS
861 levels to particle nucleation events in the Canadian Arctic, *Journal of Geophysical Research:*
862 *Atmospheres*, 116, 2011.
- 863
864 Charlson, R. J., Lovelock, J. E., Andreae, M. O., and Warren, S. G.: Oceanic phytoplankton,
865 atmospheric sulphur, cloud albedo and climate, *Nature*, 326, 655-661, 1987.

866
867 Chen, T., and Jang, M.: Secondary organic aerosol formation from photooxidation of a
868 mixture of dimethyl sulfide and isoprene, *Atmospheric Environment*, 46, 271-278, 2012.
869
870 Coello-Camba, A., Agustí, S., Holding, J., Arrieta, J. M., and Duarte, C. M.: Interactive effect
871 of temperature and CO₂ increase in Arctic phytoplankton, *Frontiers in Marine Science*, 1, 49,
872 2014.
873
874 Crawford, K. J., Brussaard, C. P. D., and Riebesell, U.: Shifts in the microbial community in
875 the Baltic Sea with increasing CO₂, *Biogeosciences Discuss.*, 2016, 1-51, 10.5194/bg-2015-
876 606, 2016.
877
878 Davidson, A. T., McKinlay, J., Westwood, K., Thompson, P., van den Enden, R., de Salas,
879 M., Wright, S., Johnson, R., and Berry, K.: Enhanced CO₂ concentrations change the
880 structure of Antarctic marine microbial communities, *Mar Ecol Prog Ser.* doi, 10, 3354, 2016.
881
882 del Valle, D. A., Kieber, D. J., Toole, D. A., Bisgrove, J., and Kiene, R. P.: Dissolved DMSO
883 production via biological and photochemical oxidation of dissolved DMS in the Ross Sea,
884 Antarctica, *Deep Sea Research Part I: Oceanographic Research Papers*, 56, 166-177,
885 <http://dx.doi.org/10.1016/j.dsr.2008.09.005>, 2009.
886
887 Egleston, E. S., Sabine, C. L., and Morel, F. M. M.: Revelle revisited: Buffer factors that
888 quantify the response of ocean chemistry to changes in DIC and alkalinity, *Global*
889 *Biogeochemical Cycles*, 24, n/a-n/a, 10.1029/2008gb003407, 2010.
890
891 Engel, A., Zondervan, I., Aerts, K., Beaufort, L., Benthien, A., Chou, L., Delille, B., Gattuso,
892 J.-P., Harlay, J., Heeman, C., Hoffman, L., Jacquet, S., Nejtgaard, J., Pizay, M.-D.,
893 Rochelle-Newall, E., Schneider, U., Terbrueggen, A., and Riebesell, U.: Testing the direct
894 effect of CO₂ concentrations on a bloom of the coccolithophorid *Emiliania huxleyi* in
895 mesocosm experiments, *Limnology and Oceanography*, 50, 493-507, 2005.
896
897 Engel, A., Schulz, K., Riebesell, U., Bellerby, R., Delille, B., and Schartau, M.: Effects of
898 CO₂ on particle size distribution and phytoplankton abundance during a mesocosm bloom
899 experiment (PeECE II), *Biogeosciences*, 5, 509-521, 2008.
900
901 Eppley, R. W.: Temperature and phytoplankton growth in the sea, *Fish. bull.*, 70, 1063-1085,
902 1972.
903
904 Fassbender, A. J., Sabine, C. L., and Feifel, K. M.: Consideration of coastal carbonate
905 chemistry in understanding biological calcification, *Geophysical Research Letters*, 43, 4467-
906 4476, 10.1002/2016gl068860, 2016.
907
908 Flynn, K. J., Blackford, J. C., Baird, M. E., Raven, J. A., Clark, D. R., Beardall, J., Brownlee,
909 C., Fabian, H., and Wheeler, G. L.: Changes in pH at the exterior surface of plankton with
910 ocean acidification, *Nature Climate Change*, 2, 510-513, 2012.
911
912 Gabric, A. J., Qu, B., Matrai, P. A., Murphy, C., Lu, H., Lin, D. R., Qian, F., and Zhao, M.:
913 Investigating the coupling between phytoplankton biomass, aerosol optical depth and sea-ice
914 cover in the Greenland Sea, *Dynamics of Atmospheres and Oceans*, 66, 94-109,
915 <http://dx.doi.org/10.1016/j.dynatmoce.2014.03.001>, 2014.

916
917 Galindo, V., Levasseur, M., Mundy, C. J., Gosselin, M., Scarratt, M., Papakyriakou, T.,
918 Stefels, J., Gale, M. A., Tremblay, J.-É., and Lizotte, M.: Contrasted sensitivity of DMSP
919 production to high light exposure in two Arctic under-ice blooms, *Journal of Experimental*
920 *Marine Biology and Ecology*, 475, 38-48, <http://dx.doi.org/10.1016/j.jembe.2015.11.009>,
921 2016.
922
923 Gattuso, J.-P., Lee, K., Rost, B., and Schulz, K.: Approaches and tools to manipulate the
924 carbonate chemistry, in: *Guide to Best Practices for Ocean Acidification Research and Data*
925 *Reporting*, edited by: Riebesell, U., Fabry, V. J., Hansson, L., and Gattuso, J. P.,
926 Publications Office of the European Union, Luxembourg, 263, 2010.
927
928 Gattuso, J.-P., Magnan, A., Bille, R., Cheung, W., Howes, E., Joos, F., Allemand, D., Bopp,
929 L., Cooley, S., and Eakin, C.: Contrasting futures for ocean and society from different
930 anthropogenic CO₂ emissions scenarios, *Science*, 349, aac4722, 2015.
931
932 Hagens, M., and Middelburg, J. J.: Attributing seasonal pH variability in surface ocean
933 waters to governing factors, *Geophysical Research Letters*, 43, 12,528-512,537,
934 [doi:10.1002/2016GL071719](https://doi.org/10.1002/2016GL071719), 2016.
935
936 Hauri, C., Friedrich, T., and Timmermann, A.: Abrupt onset and prolongation of aragonite
937 undersaturation events in the Southern Ocean, *Nature Clim. Change*, 6, 172-176,
938 [10.1038/nclimate2844](https://doi.org/10.1038/nclimate2844)
939 [http://www.nature.com/nclimate/journal/v6/n2/abs/nclimate2844.html#supplementary-](http://www.nature.com/nclimate/journal/v6/n2/abs/nclimate2844.html#supplementary-information)
940 [information](http://www.nature.com/nclimate/journal/v6/n2/abs/nclimate2844.html#supplementary-information), 2016.
941
942 Holding, J. M., Duarte, C. M., Sanz-Martin, M., Mesa, E., Arrieta, J. M., Chierici, M.,
943 Hendriks, I. E., Garcia-Corral, L. S., Regaudie-de-Gioux, A., Delgado, A., Reigstad, M.,
944 Wassmann, P., and Agusti, S.: Temperature dependence of CO₂-enhanced primary
945 production in the European Arctic Ocean, *Nature Climate Change*, 5, 1079,
946 [10.1038/nclimate2768](https://doi.org/10.1038/nclimate2768), 2015.
947
948 Hönisch, B., Ridgwell, A., Schmidt, D. N., Thomas, E., Gibbs, S. J., Sluijs, A., Zeebe, R.,
949 Kump, L., Martindale, R. C., Greene, S. E., Kiessling, W., Ries, J., Zachos, J. C., Royer, D.
950 L., Barker, S., Marchitto, T. M., Moyer, R., Pelejero, C., Ziveri, P., Foster, G. L., and
951 Williams, B.: The Geological Record of Ocean Acidification, *Science*, 335, 1058-1063,
952 [10.1126/science.1208277](https://doi.org/10.1126/science.1208277), 2012.
953
954 Hopkins, F. E., Turner, S. M., Nightingale, P. D., Steinke, M., Bakker, D., and Liss, P. S.:
955 Ocean acidification and marine trace gas emissions, *Proceedings of the National Academy of*
956 *Sciences*, 107, 760-765, 2010.
957
958 Hopkins, F. E., and Archer, S. D.: Consistent increase in dimethyl sulfide (DMS) in response
959 to high CO₂ in five shipboard bioassays from contrasting NW European waters,
960 *Biogeosciences*, 11, 4925-4940, [10.5194/bg-11-4925-2014](https://doi.org/10.5194/bg-11-4925-2014), 2014.
961
962

963 Hoppe, C. J., Schuback, N., Semeniuk, D. M., Maldonado, M. T., and Rost, B.: Functional
964 Redundancy Facilitates Resilience of Subarctic Phytoplankton Assemblages toward Ocean
965 Acidification and High Irradiance, *Frontiers in Marine Science*, 4, 229, 2017.
966
967 Hoppe, C. J. M., Hassler, C. S., Payne, C. D., Tortell, P. D., Rost, B., and Trimborn, S.: Iron
968 Limitation Modulates Ocean Acidification Effects on Southern Ocean Phytoplankton
969 Communities, *PLOS ONE*, 8, e79890, 10.1371/journal.pone.0079890, 2013.
970
971 Hoppe, C. J. M., Wolf, K. K. E., Schuback, N., Tortell, P. D., and Rost, B.: Compensation of
972 ocean acidification effects in Arctic phytoplankton assemblages, *Nature Climate Change*, 8,
973 529-533, 10.1038/s41558-018-0142-9, 2018.
974
975 Husherr, R., Levasseur, M., Lizotte, M., Tremblay, J.-É., Mol, J., Helmuth, T., Gosselin, M.,
976 Starr, M., Miller, L. A., and Jarníková, T.: Impact of ocean acidification on Arctic
977 phytoplankton blooms and dimethyl sulfide concentration under simulated ice-free and
978 under-ice conditions, *Biogeosciences*, 14, 2407, 2017.
979
980 Jarníková, T., and Tortell, P. D.: Towards a revised climatology of summertime
981 dimethylsulfide concentrations and sea–air fluxes in the Southern Ocean, *Environ. Chem.*, 13,
982 364-378, <http://dx.doi.org/10.1071/EN14272>, 2016.
983
984 Johnson, M. T., and Bell, T. G.: Coupling between dimethylsulfide emissions and the ocean-
985 atmosphere exchange of ammonia, *Environ. Chem.*, 5, 259-267, doi:10.1071/EN08030, 2008.
986
987 Kapsenberg, L., Kelley, A. L., Shaw, E. C., Martz, T. R., and Hofmann, G. E.: Near-shore
988 Antarctic pH variability has implications for the design of ocean acidification experiments,
989 *Scientific Reports*, 5, 9638, 10.1038/srep09638, 2015.
990
991 Kiene, R. P., and Slezak, D.: Low dissolved DMSP concentrations in seawater revealed by
992 small-volume gravity filtration and dialysis sampling *Limnology and Oceanography*
993 *Methods*, 4, 80-95, 2006.
994
995 Kim, J. M., Lee, K., Shin, K., Kang, J. H., Lee, H. W., Kim, M., Jang, P. G., and Jang, M. C.:
996 The effect of seawater CO₂ concentration on growth of a natural phytoplankton assemblage
997 in a controlled mesocosm experiment, *Limnology and Oceanography*, 51, 1629-1636, 2006.
998
999 Kim, J. M., Lee, K., Yang, E. J., Shin, K., Noh, J. H., Park, K. T., Hyun, B., Jeong, H. J.,
1000 Kim, J. H., Kim, K. Y., Kim, M., Kim, H. C., Jang, P. G., and Jang, M. C.: Enhanced
1001 Production of Oceanic Dimethylsulfide Resulting from CO₂-Induced Grazing Activity in a
1002 High CO₂ World, *Environmental Science & Technology*, 44, 8140-8143,
1003 10.1021/es102028k, 2010.
1004
1005 Kitidis, V., Hardman-Mountford, N. J., Litt, E., Brown, I., Cummings, D., Hartman, S.,
1006 Hydes, D., Fishwick, J. R., Harris, C., and Martinez-Vicente, V.: Seasonal dynamics of the
1007 carbonate system in the Western English Channel, *Continental Shelf Research*, 42, 30-40,
1008 2012.
1009
1010 Korhonen, H., Carslaw, K. S., Spracklen, D. V., Mann, G. W., and Woodhouse, M. T.:
1011 Influence of oceanic dimethyl sulfide emissions on cloud condensation nuclei concentrations

1012 and seasonality over the remote Southern Hemisphere oceans: A global model study, *Journal*
1013 *of Geophysical Research-Atmospheres*, 113, 16, D1520410.1029/2007jd009718, 2008a.
1014
1015 Korhonen, H., Carslaw, K. S., Spracklen, D. V., Ridley, D. A., and Ström, J.: A global model
1016 study of processes controlling aerosol size distributions in the Arctic spring and summer,
1017 *Journal of Geophysical Research*, 113, D08211, 2008b.
1018
1019 Lana, A., Bell, T. G., Simó, R., Vallina, S. M., Ballabrera-Poy, J., Kettle, A. J., Dachs, J.,
1020 Bopp, L., Saltzman, E. S., Stefels, J., Johnson, J. E., and Liss, P. S.: An updated climatology
1021 of surface dimethylsulfide concentrations and emission fluxes in the global ocean, *Global*
1022 *Biogeochem. Cycles*, 25, GB1004, 2011.
1023
1024 Leaitch, W. R., Sharma, S., Huang, L., Toom-Saunty, D., Chivulescu, A., Macdonald, A.
1025 M., von Salzen, K., Pierce, J. R., Bertram, A. K., and Schroder, J. C.: Dimethyl sulfide
1026 control of the clean summertime Arctic aerosol and cloud, *Elementa: Science of the*
1027 *Anthropocene*, 1, 000017, 2013.
1028
1029 Leakey, R.: *Effect of Ocean Acidification on Arctic Surface Ocean Biology,*
1030 *Biogeochemistry and Climate*, British Oceanographic Data Centre, 2012.
1031 Levasseur, M.: Impact of Arctic meltdown on the microbial cycling of sulphur, *Nature*
1032 *Geoscience*, 6, 691-700, 2013.
1033
1034 Lewis, E., and Wallace, D. W. R.: *Program Developed for CO2 System Calculations*, Carbon
1035 *Dioxide Information Analysis Center*, Oak Ridge National Laboratory, U.S. Department of
1036 *Energy*, Oak Ridge, Tennessee., 1998.
1037
1038 McCoy, D. T., Burrows, S. M., Wood, R., Grosvenor, D. P., Elliott, S. M., Ma, P.-L., Rasch,
1039 P. J., and Hartmann, D. L.: Natural aerosols explain seasonal and spatial patterns of Southern
1040 *Ocean cloud albedo*, *Science Advances*, 1, 10.1126/sciadv.1500157, 2015.
1041
1042 McNeil, B. I., and Matear, R. J.: Southern Ocean acidification: A tipping point at 450-ppm
1043 *atmospheric CO2*, *Proceedings of the National Academy of Sciences*, 105, 18860-18864,
1044 2008.
1045
1046 Menzo, Z., Elliott, S., Hartin, C., Hoffman, F., and Wang, S.: Climate change impacts on
1047 *natural sulfur production: Ocean acidification and community shifts*, *Atmosphere*, 9, 167,
1048 2018.
1049
1050 Monier, A., Findlay, H. S., Charvet, S., and Lovejoy, C.: Late winter under ice pelagic
1051 *microbial communities in the high Arctic Ocean and the impact of short-term exposure to*
1052 *elevated CO2 levels*, *Name: Frontiers in Microbiology*, 5, 490, 2014.
1053
1054 Orr, J. C., Fabry, V. J., Aumont, O., Bopp, L., Doney, S. C., Feely, R. A., Gnanadesikan, A.,
1055 *Gruber, N., Ishida, A., and Joos, F.: Anthropogenic ocean acidification over the twenty-first*
1056 *century and its impact on calcifying organisms*, *Nature*, 437, 681-686, 2005.
1057
1058 Park, K.-T., Lee, K., Shin, K., Yang, E. J., Hyun, B., Kim, J.-M., Noh, J. H., Kim, M., Kong,
1059 *B., Choi, D. H., Choi, S.-J., Jang, P.-G., and Jeong, H. J.: Direct Linkage between Dimethyl*
1060 *Sulfide Production and Microzooplankton Grazing, Resulting from Prey Composition*

1061 Change under High Partial Pressure of Carbon Dioxide Conditions, *Environmental Science &*
1062 *Technology*, 48, 4750-4756, 10.1021/es403351h, 2014.

1063

1064 Poulton, A. J., Daniels, C. J., Esposito, M., Humphreys, M. P., Mitchell, E., Ribas-Ribas, M.,
1065 Russell, B. C., Stinchcombe, M. C., Tynan, E., and Richier, S.: Production of dissolved
1066 organic carbon by Arctic plankton communities: Responses to elevated carbon dioxide and
1067 the availability of light and nutrients, *Deep Sea Research Part II: Topical Studies in*
1068 *Oceanography*, 127, 60-74, <http://dx.doi.org/10.1016/j.dsr2.2016.01.002>, 2016.

1069

1070 Raven, J., Caldeira, K., Elderfield, H., Hoegh-Guldberg, O., Liss, P., Riebesell, U., Shepherd,
1071 J., Turley, C., and Watson, A.: Ocean acidification due to increasing atmospheric carbon
1072 dioxide, *The Royal Society, Policy Document 12/05*, London, 2005.

1073

1074 Rempillo, O., Seguin, A. M., Norman, A. L., Scarratt, M., Michaud, S., Chang, R., Sjostedt,
1075 S., Abbatt, J., Else, B., and Papakyriakou, T.: Dimethyl sulfide air-sea fluxes and biogenic
1076 sulfur as a source of new aerosols in the Arctic fall, *Journal of Geophysical Research:*
1077 *Atmospheres*, 116, 2011.

1078

1079 Revelle, R., and Suess, H. E.: Carbon Dioxide Exchange Between Atmosphere and Ocean
1080 and the Question of an Increase of Atmospheric CO₂ during the Past Decades, *Tellus A*, 9,
1081 1957.

1082

1083 Richier, S., Achterberg, E. P., Dumousseaud, C., Poulton, A. J., Suggett, D. J., Tyrrell, T.,
1084 Zubkov, M. V., and Moore, C. M.: Phytoplankton responses and associated carbon cycling
1085 during shipboard carbonate chemistry manipulation experiments conducted around Northwest
1086 European shelf seas, *Biogeosciences*, 11, 4733-4752, 10.5194/bg-11-4733-2014, 2014.

1087

1088 Richier, S., Achterberg, E. P., Humphreys, M. P., Poulton, A. J., Suggett, D. J., Tyrrell, T.,
1089 and Moore, C. M.: Geographical CO₂ sensitivity of phytoplankton correlates with ocean
1090 buffer capacity, *Global Change Biology*, doi:10.1111/gcb.14324, 2018.

1091

1092 Riebesell, U., Gattuso, J. P., Thingstad, T. F., and Middelburg, J. J.: Preface "Arctic ocean
1093 acidification: pelagic ecosystem and biogeochemical responses during a mesocosm study",
1094 *Biogeosciences*, 10, 5619-5626, 10.5194/bg-10-5619-2013, 2013a.

1095

1096 Riebesell, U., J. Czerny, K. von Bröckel, T. Boxhammer, J. Büdenbender, M. Deckelnick, M.
1097 Fischer et al.: Technical Note: a mobile sea-going mesocosm system-new opportunities for
1098 ocean change research. *Biogeosciences* 10, 1835e1847, 2013b.

1099 Rysgaard, S., Glud, R. N., Lennert, K., Cooper, M., Halden, N., Leakey, R., Hawthorne, F.,
1100 and Barber, D.: Ikaite crystals in melting sea ice-implications for pCO₂ and pH levels in
1101 Arctic surface waters, *The Cryosphere*, 6, 901, 2012.

1102

1103 Sabine, C. L., Feely, R. A., Gruber, N., Key, R. M., Lee, K., Bullister, J. L., Wanninkhof, R.,
1104 Wong, C. S., Wallace, D. W. R., Tilbrook, B., Millero, F. J., Peng, T.-H., Kozyr, A., Ono, T.,
1105 and Rios, A. F.: The oceanic sink for anthropogenic CO₂, *Science*, 305, 367-371, 2004.

1106

1107 Schoemann, V., Becquevort, S., Stefels, J., Rousseau, V., and Lancelot, C.: Phaeocystis
1108 blooms in the global ocean and their controlling mechanisms: a review, *Journal of Sea*
1109 *Research*, 53, 43-66, 2005.

1110

1111 Schulz, K. G., Riebesell, U., Bellerby, R. G. J., Biswas, H., Meyerhofer, M., Muller, M. N.,
1112 Egge, J. K., Nejstgaard, J. C., Neill, C., Wohlers, J., and Zollner, E.: Build-up and decline of
1113 organic matter during PeECE III, *Biogeosciences*, 5, 707-718, 2008.

1114
1115 Schulz, K. G., Bellerby, R. G. J., Brussaard, C. P. D., Büdenbender, J., Czerny, J., Engel, A.,
1116 Fischer, M., Koch-Klavnsen, S., Krug, S. A., Lischka, S., Ludwig, A., Meyerhöfer, M.,
1117 Nondal, G., Silyakova, A., Stuhr, A., and Riebesell, U.: Temporal biomass dynamics of an
1118 Arctic plankton bloom in response to increasing levels of atmospheric carbon dioxide,
1119 *Biogeosciences*, 10, 161-180, 10.5194/bg-10-161-2013, 2013.

1120
1121 Schwinger, J., Tjiputra, J., Goris, N., Six, K. D., Kirkevåg, A., Seland, Ø., Heinze, C., and
1122 Ilyina, T.: Amplification of global warming through pH-dependence of DMS-production
1123 simulated with a fully coupled Earth system model (under review in *Biogeosciences*, doi:
1124 10.5194/bg-2017-33), *Biogeosciences*, 2017.

1125
1126 Sharma, S., Chan, E., Ishizawa, M., Toom-Sauntry, D., Gong, S., Li, S., Tarasick, D.,
1127 Leaitch, W., Norman, A., and Quinn, P.: Influence of transport and ocean ice extent on
1128 biogenic aerosol sulfur in the Arctic atmosphere, *Journal of Geophysical Research:
1129 Atmospheres*, 117, 2012.

1130
1131 Six, K. D., Kloster, S., Ilyina, T., Archer, S. D., Zhang, K., and Maier-Reimer, E.: Global
1132 warming amplified by reduced sulphur fluxes as a result of ocean acidification, *Nature
1133 Climate Change*, 3, 975, 2013.

1134
1135 Stefels, J.: Physiological aspects of the production and conversion of DMSP in marine algae
1136 and higher plants, *Journal of Sea Research*, 43, 183-197, 2000.

1137
1138 Steinacher, M., Joos, F., Frolicher, T. L., Plattner, G. K., and Doney, S. C.: Imminent ocean
1139 acidification in the Arctic projected with the NCAR global coupled carbon cycle-climate
1140 model, *Biogeosciences*, 6, 515-533, 2009.

1141
1142 Stillman, J. H., and Paganini, A. W.: Biochemical adaptation to ocean acidification, *Journal
1143 of Experimental Biology*, 218, 1946-1955, 10.1242/jeb.115584, 2015.

1144
1145 Sunda, W., Kieber, D. J., Kiene, R. P., and Huntsman, S.: An antioxidant function for DMSP
1146 and DMS in marine algae, *Nature*, 418, 317-320, 2002.

1147
1148 Tarling, G.: Sea Surface Ocean Acidification Consortium Cruise to the Southern Ocean,
1149 British Oceanographic Data Centre, 2013.

1150
1151 Thoisen, C., Riisgaard, K., Lundholm, N., Nielsen, T. G., and Hansen, P. J.: Effect of
1152 acidification on an Arctic phytoplankton community from Disko Bay, West Greenland,
1153 *Marine Ecology Progress Series*, 520, 21-34, 2015.

1154
1155 Thomas, D. N., and Dieckmann, G. S.: Antarctic Sea Ice--a Habitat for Extremophiles,
1156 *Science*, 295, 641-644, 10.1126/science.1063391, 2002.

1157
1158 Thomson, P. G., Davidson, A. T., and Maher, L.: Increasing CO₂ changes community
1159 composition of pico- and nano-sized protists and prokaryotes at a coastal Antarctic site,
1160 *Marine Ecology Progress Series*, 554, 51-69, 2016.

1161
1162 Tortell, P. D., Payne, C. D., Li, Y., Trimborn, S., Rost, B., Smith, W. O., Riesselman, C.,
1163 Dunbar, R. B., Sedwick, P., and DiTullio, G. R.: CO₂ sensitivity of Southern Ocean
1164 phytoplankton, *Geophysical Research Letters*, 35, 2008.
1165
1166 Trimborn, S., Brenneis, T., Hoppe, C. J. M., Laglera, L. M., Norman, L., Santos-Echeandía,
1167 J., Völkner, C., Wolf-Gladrow, D., and Hassler, C. S.: Iron sources alter the response of
1168 Southern Ocean phytoplankton to ocean acidification, *Marine Ecology Progress Series*, 578,
1169 35-50, 2017.
1170
1171 Tynan, E., Clarke, J. S., Humphreys, M. P., Ribas-Ribas, M., Esposito, M., Rérolle, V. M. C.,
1172 Schlosser, C., Thorpe, S. E., Tyrrell, T., and Achterberg, E. P.: Physical and biogeochemical
1173 controls on the variability in surface pH and calcium carbonate saturation states in the
1174 Atlantic sectors of the Arctic and Southern Oceans, *Deep Sea Research Part II: Topical
1175 Studies in Oceanography*, 127, 7-27, <http://dx.doi.org/10.1016/j.dsr2.2016.01.001>, 2016.
1176
1177 Vogt, M., Steinke, M., Turner, S., Paulino, A., Meyerhöfer, M., Riebesell, U., LeQuéré, C.,
1178 and Liss, P.: Dynamics of dimethylsulphoniopropionate and dimethylsulphide under different
1179 CO₂ concentrations during a mesocosm experiment, *Biogeosciences*, 5, 407-419, 2008.
1180
1181 von Glasow, R., and Crutzen, P. J.: Model study of multiphase DMS oxidation with a focus
1182 on halogens, *Atmos. Chem. Phys.*, 4, 589-608, 2004.
1183
1184 Webb, A. L., Malin, G., Hopkins, F. E., Ho, K. L., Riebesell, U., Schulz, K. G., Larsen, A.,
1185 and Liss, P. S.: Ocean acidification has different effects on the production of dimethylsulfide
1186 and dimethylsulfoniopropionate measured in cultures of *Emiliana huxleyi* and a mesocosm
1187 study: a comparison of laboratory monocultures and community interactions, *Environ.
1188 Chem.*, -, <http://dx.doi.org/10.1071/EN14268>, 2015.
1189
1190 Webb, A. L., Leedham-Elvidge, E., Hughes, C., Hopkins, F. E., Malin, G., Bach, L. T.,
1191 Schulz, K., Crawford, K., Brussaard, C. P. D., Stühr, A., Riebesell, U., and Liss, P. S.: Effect
1192 of ocean acidification and elevated fCO₂ on trace gas production by a Baltic Sea summer
1193 phytoplankton community, *Biogeosciences*, 13, 4595-4613, [10.5194/bg-13-4595-2016](https://doi.org/10.5194/bg-13-4595-2016), 2016.
1194
1195 Woodhouse, M. T., Mann, G. W., Carslaw, K. S., and Boucher, O.: Sensitivity of cloud
1196 condensation nuclei to regional changes in dimethyl-sulphide emissions, *Atmos. Chem.
1197 Phys.*, 13, 2723-2733, [10.5194/acp-13-2723-2013](https://doi.org/10.5194/acp-13-2723-2013), 2013.

1198 Table 1. Summary of the station locations and characteristic of the water sampled for the 18 microcosm experiments performed in temperate,
 1199 sub-polar and polar waters. All polar stations were sampled for JR271 and JR274, with the exception of NS and IB.

Cruise	Station ID	Location	Sampling location	Sampling date	Sampling depth (m)	SST (°C)	Salinity	Nitrate (uM)	Total Chl <i>a</i> ($\mu\text{g L}^{-1}$)	chl _{>10 μm} : chl _{total}	pCO ₂ (μatm) T ₀	pH (total) T ₀	Experimental timepoints T ₁ , T ₂ (hours)	Reference
D366	E01	Mingulay Reef	56°47.688N 7°24.300W	8 June 2011	6	11.3	34.8	1.1	3.3	no data	334.9	8.1	48, 96	<i>Hopkins & Archer (2011)</i>
	E02	Irish Sea	52°28.237N 5°54.052W	14 June 2011	5	11.8	34.4	0.3	3.5	0.80 ± 0.03	329.3	8.1	48, 96	<i>Hopkins & Archer (2011)</i>
	E02b	Bay of Biscay	46°29.794N 7°12.355W	19 June 2011	5	14.5	35.6	0.9	1.8	no data	340.3	8.1	48	<i>This study</i>
	E03	Bay of Biscay	46°12.137N 7°13.253W	21 June 2011	10	15.3	35.8	0.6	0.8	0.43 ± 0.03	323.9	8.1	48, 96	<i>Hopkins & Archer (2011)</i>
	E04	Southern North Sea	52°59.661N 2°29.841E	26 June 2011	5	14.6	34.1	0.9	1.3	0.19 ± 0.02	399.8	8.0	48, 96	<i>Hopkins & Archer (2011)</i>
	E04b	Mid North Sea	57°45.729N 4°35.434E	29 June 2011	5	13.2	34.8	No data	0.5	0.14 ± 0.003	327.3	8.1	48	<i>This study</i>
	E05	Mid North Sea	56°30.293N 3°39.506E	2 July 2011	12	14.0	35.0	0.2	0.3	0.23 ± 0.01	360.2	8.1	48, 96	<i>Hopkins & Archer (2011)</i>
	E05b	Atlantic Ocean	59°40.721N 4°07.633E	3 July 2011	4	13.4	30.7	0.3	0.7	0.12 ± 0.01	310.7	8.1	48	<i>This study</i>
	E06	Atlantic Ocean	59°59.011N 2°30.896E	3 July 2011	4	12.5	34.9	0.4	1.1	0.14 ± 0.01	287.1	8.2	48	<i>This study</i>
JR271	NS	Mid North Sea	56°15.59N 2°37.59E	3 June 2012	15	10.8	35.1	0.04	0.3	0.52 ± 0.05	300.5	8.2	48, 96	<i>This study</i>
	IB	Iceland Basin	60°35.39N 18°51.23W	8 June 2012	7	10.7	35.2	5.0	1.8	0.27 ± 0.02	309.7	8.1	48, 96	<i>This study</i>
	GG-AO	Greenland Gyre	76°10.52 N 2°32.96 W	13 June 2012	5	1.7	34.9	9.3	1.0	0.34 ± 0.001	289.3	8.2	48, 96	<i>This study</i>
	GI-AO	Greenland ice edge	78°21.15 N 3°39.85 W	18 June 2012	5	-1.6	32.6	4.2	2.7	0.78 ± 0.03	304.7	8.1	48, 96	<i>This study</i>
	BS-AO	Barents Sea	72°53.49 N 26°00.09 W	24 June 2012	5	6.6	35.0	5.4	1.3	0.04 ± 0.01	304.3	8.1	48, 96	<i>This study</i>
JR274	DP-SO	Drake Passage	58°22.00 S 56°15.12 W	13 Jan 2013	8	1.9	33.2	22.0	2.4	1.00 ± 0.06	279.3	8.2	48, 96	<i>This study</i>
	WS-SO	Weddell Sea	60°58.55 S 48°05.19 W	18 Jan 2013	6	-1.4	33.6	24.9	0.6	0.67 ± 0.06	510.5	7.9	72, 144	<i>This study</i>
	SG-SO	South Georgia	52°41.36 S 36°37.28 W	25 Jan 2013	5	2.2	33.9	24.1	0.7	0.35 ± 0.04	342.6	8.1	72, 144	<i>This study</i>
	SS-SO	South Sandwich	58°05.13 S 25°55.55 W	1 Feb 2013	7	0.5	33.7	18.5	4.6	0.57 ± 0.02	272.6	8.2	96, 168	<i>This study</i>

1200 Table 2. Mean (\pm SD) ratio of $>10\mu\text{m}$ Chl a to total Chl a ($\text{chl}_{>10\mu\text{m}}:\text{chl}_{\text{total}}$) for polar
 1201 microcosm sampling stations. * indicates significant difference from the response to ambient
 1202 CO_2 . Exact CO_2 treatments are down in Figure 3 and 4.

Station	Time	Ambient	Mid CO_2	High CO_2	High+ CO_2	High++ CO_2
GG	48 h	0.3 ± 0.1	0.3 ± 0.03	0.4 ± 0.2	0.3 ± 0.1	N/A
	96 h	1.0 ± 0.02	0.9 ± 0.2	0.8 ± 0.1	0.7 ± 0.2	
GI	48 h	1.0 ± 0.1	1.0 ± 0.1	0.8 ± 0.1	1.0 ± 0.0	N/A
	96 h	1.0 ± 0.1	1.1 ± 0.1	0.8 ± 0.1	0.8 ± 0.1	
BS	48 h	0.02 ± 0.01	0.04 ± 0.01	0.03 ± 0.01	0.02 ± 0.01	N/A
	96 h	0.04 ± 0.01	0.05 ± 0.04	0.05 ± 0.04	0.04 ± 0.04	
DP	48 h	1.0 ± 0.3	N/A	1.0 ± 0.1	N/A	N/A
	96 h	0.9 ± 0.1		1.0 ± 0.1		
WS	72 h	0.6 ± 0.1	N/A	0.7 ± 0.1	N/A	N/A
	144 h	0.7 ± 0.1		0.7 ± 0.1		
SG	72 h	0.3 ± 0.02	N/A	0.4 ± 0.1	0.3 ± 0.1	0.4 ± 0.03
	144 h	0.5 ± 0.1		0.6 ± 0.04	0.5 ± 0.1	0.4 ± 0.03
SS	96 h	0.7 ± 0.04	N/A	$1.5 \pm 0.1^*$	0.7 ± 0.02	$1.6 \pm 0.1^*$
	168 h	0.9 ± 0.2		$1.4 \pm 0.02^*$	0.8 ± 0.004	$1.4 \pm 0.2^*$

1203

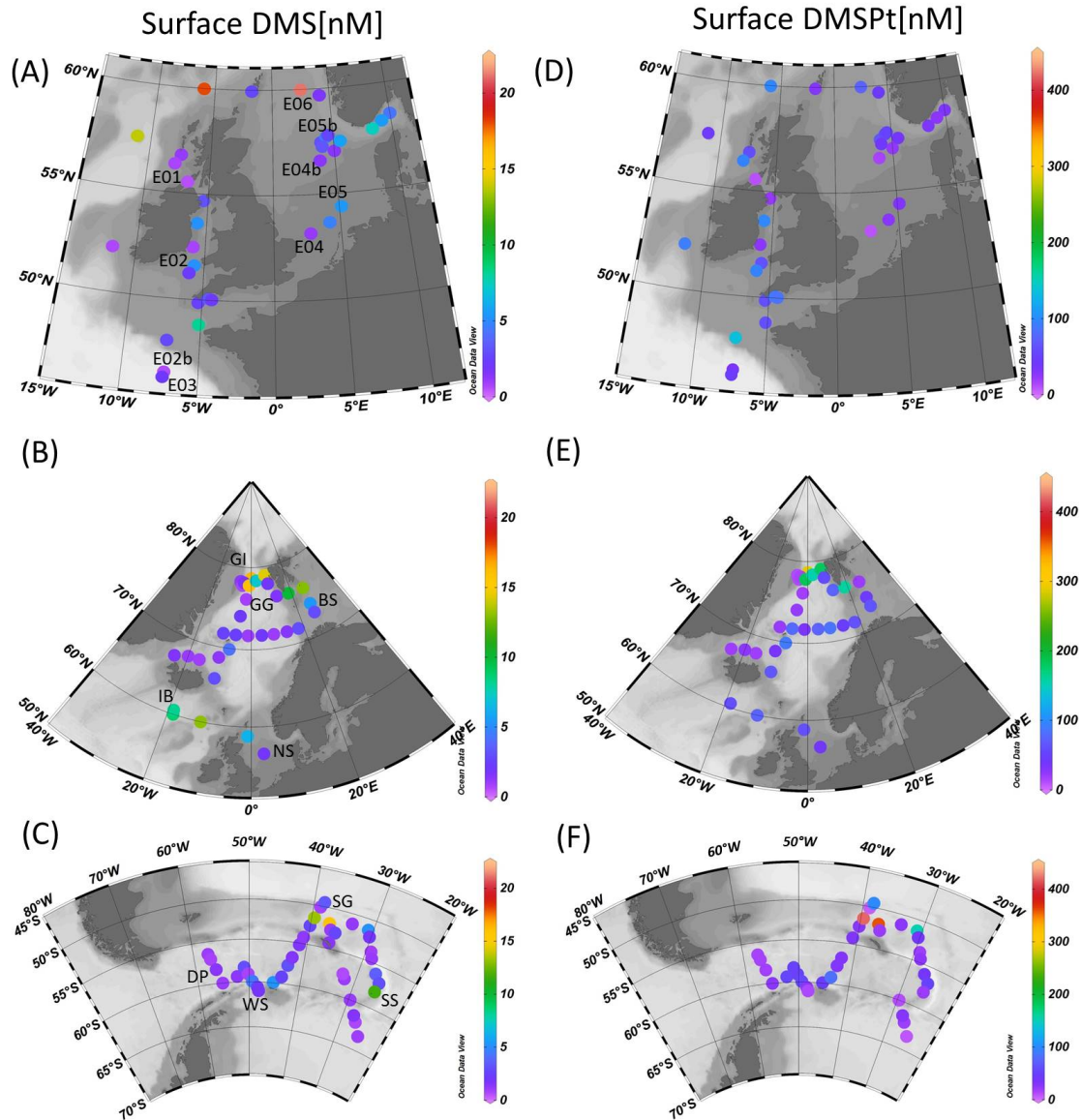
1204 Table 3. DMS and DMSPt response (mean \pm SD, $n = 3$) to high CO_2 treatments during
 1205 previously unpublished small-scale experiments from the NW European shelf cruise D366.
 1206 For details of sampling stations, see Table 1.

	0 h Ambient	48 h Ambient	48 h Mid CO_2	48 h High CO_2	96 h Ambient	96 h Mid CO_2	96 h High CO_2
DMS (nM)							
<i>E02b</i>	2.4 ± 0.3	2.1 ± 0.6		2.7 ± 0.6			
<i>E04b</i>		6.4 ± 1.4		14.7 ± 8.1			
<i>E05b</i>		3.3 ± 0.1		4.5 ± 0.6			
<i>E06</i>	18.7 ± 0.5	18.1	24.2	25.2	18.1	24.2	25.3
DMSPt (nM)							
<i>E02b</i>		49.5 ± 2.0		26.4 ± 2.9			
<i>E04b</i>		68.2 ± 10.3		36.8 ± 7.5			
<i>E05b</i>		48.7 ± 11.2		37.4 ± 4.8			
<i>E06</i>	76.7 ± 5.7	114.6	98.43	108.5	20.4	30.7	32.0

1207

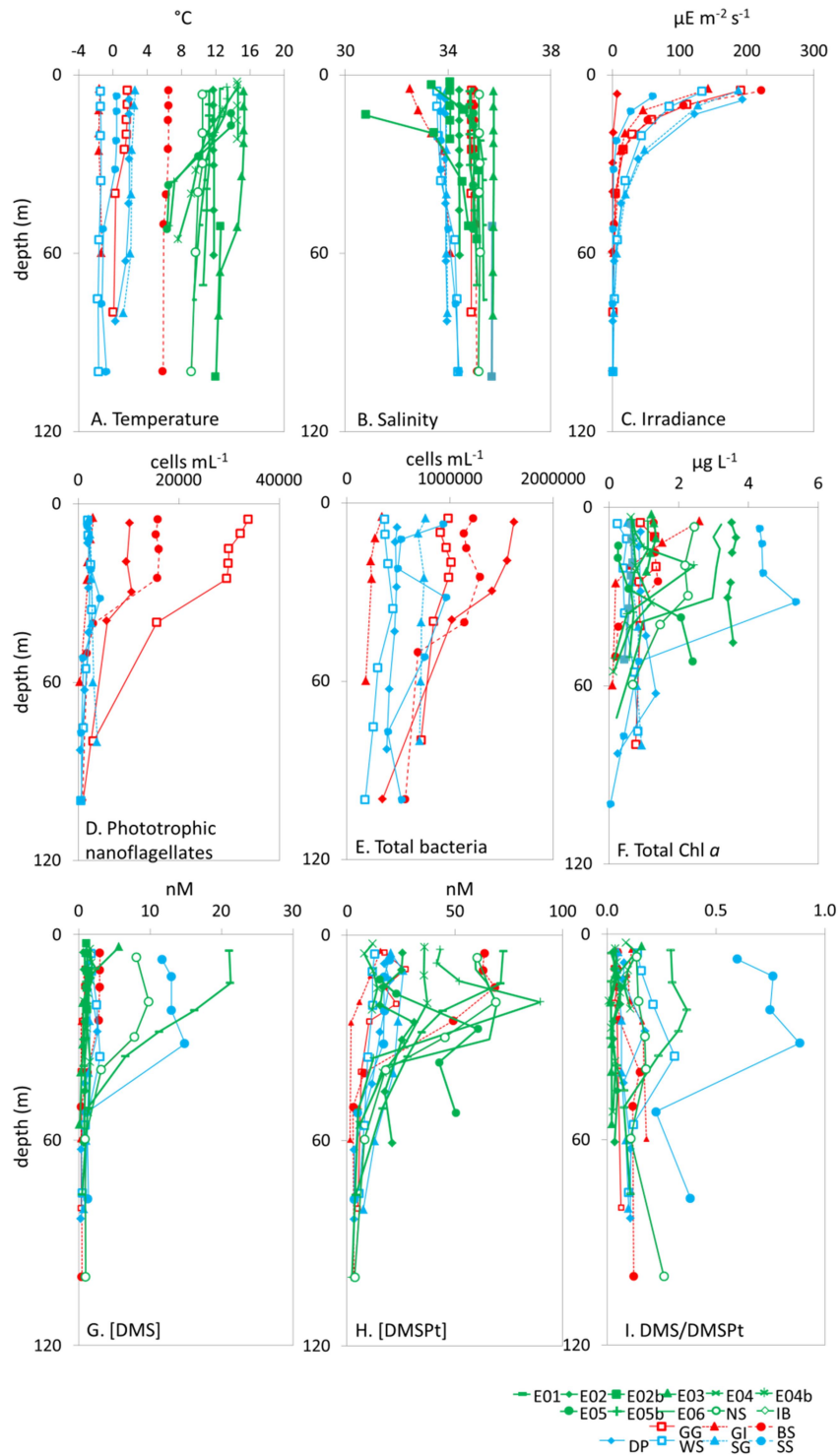
1208

1209



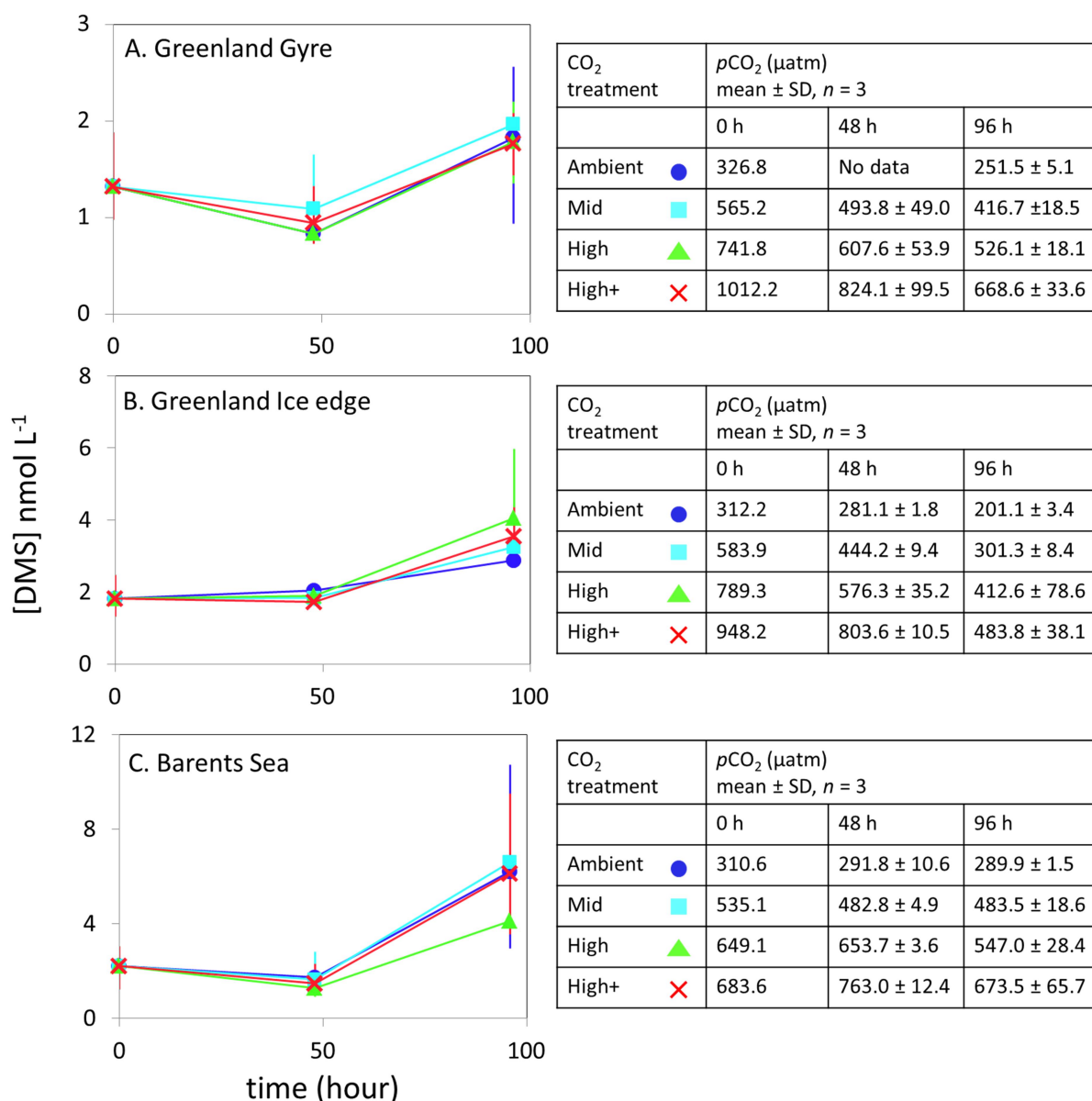
1210

1211 Figure 1. Surface (<5 m) concentrations (nM) of DMS (A-C) and total DMSP (D-F) for
 1212 cruises in the NW European shelf (D366) (A,D), the sub-Arctic and Arctic Ocean (JR271)
 1213 (B,E) and the Southern Ocean (JR274) (C,F). Locations of sampling stations for microcosm
 1214 experiments shown in letters/numbers. E01 – E05: see Hopkins & Archer 2014. NS = *North*
 1215 *Sea*, IB = *Iceland Basin*, GI = *Greenland Ice-edge*, GG = *Greenland Gyre*, BS = *Barents Sea*,
 1216 DP = *Drake Passage*, WS = *Weddell Sea*, SG = *South Georgia*, SS = *South Sandwich*.



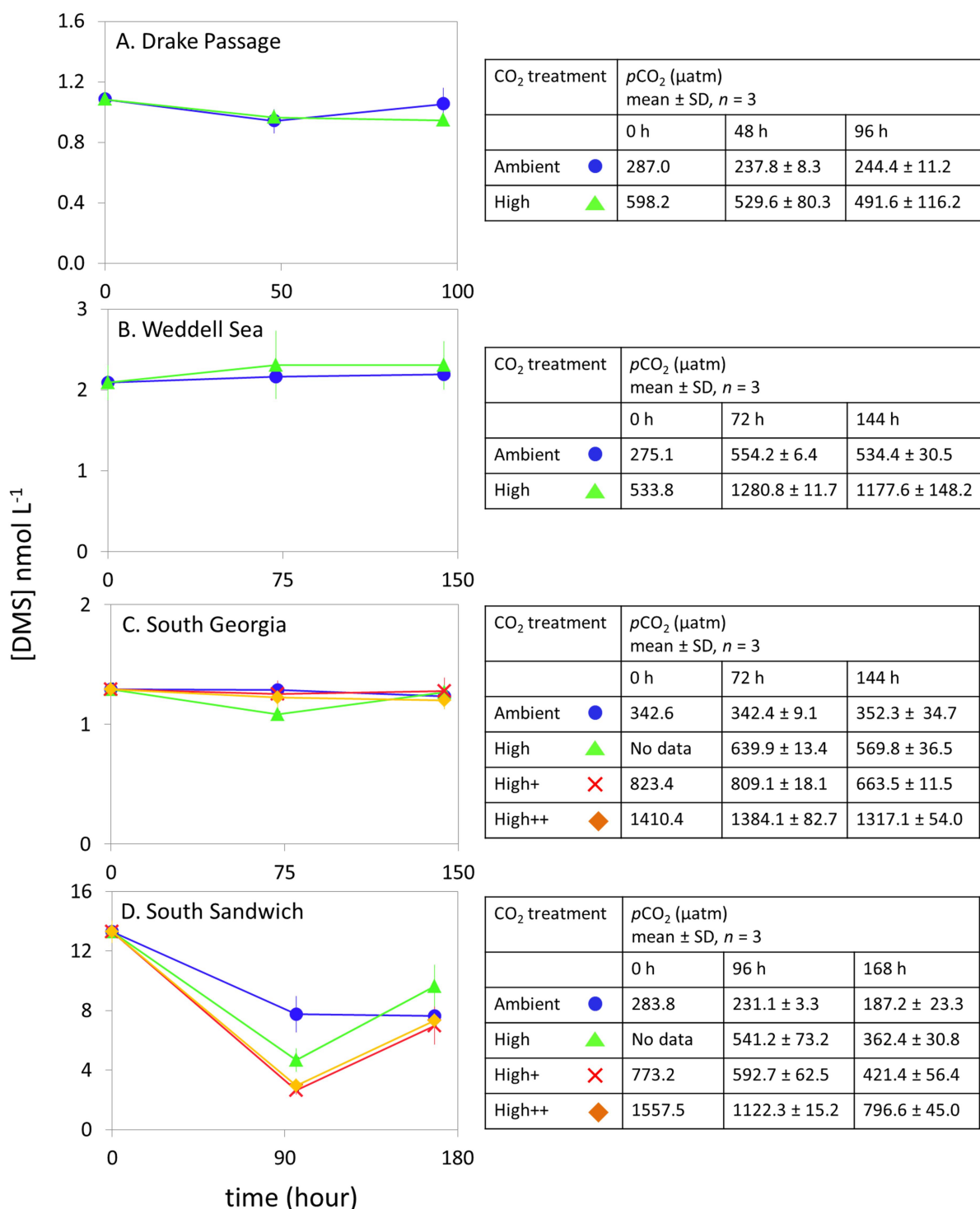
1217

1218 Figure 2. Depth profiles down to 100 m depth for all 18 sampling stations showing A.
 1219 Temperature ($^{\circ}\text{C}$), B. Salinity, C. Irradiance ($\mu\text{E m}^{-2} \text{s}^{-1}$), D. phototrophic nanoflagellate
 1220 abundance (cells mL^{-1}), E. total bacteria abundance (cells mL^{-1}), F. total Chl a ($\mu\text{g L}^{-1}$), G.
 1221 [DMS] (nM), H. total [DMSPt] (nM) and I. DMS/DMSPt from CTD casts at sampling
 1222 stations for microcosm experiments in temperate (green), Arctic (red) and Southern Ocean
 1223 (blue) waters. See Table 1 for station details. Data for irradiance, phototrophic
 1224 nanoflagellates and total bacteria were not collected for temperate stations.



1226

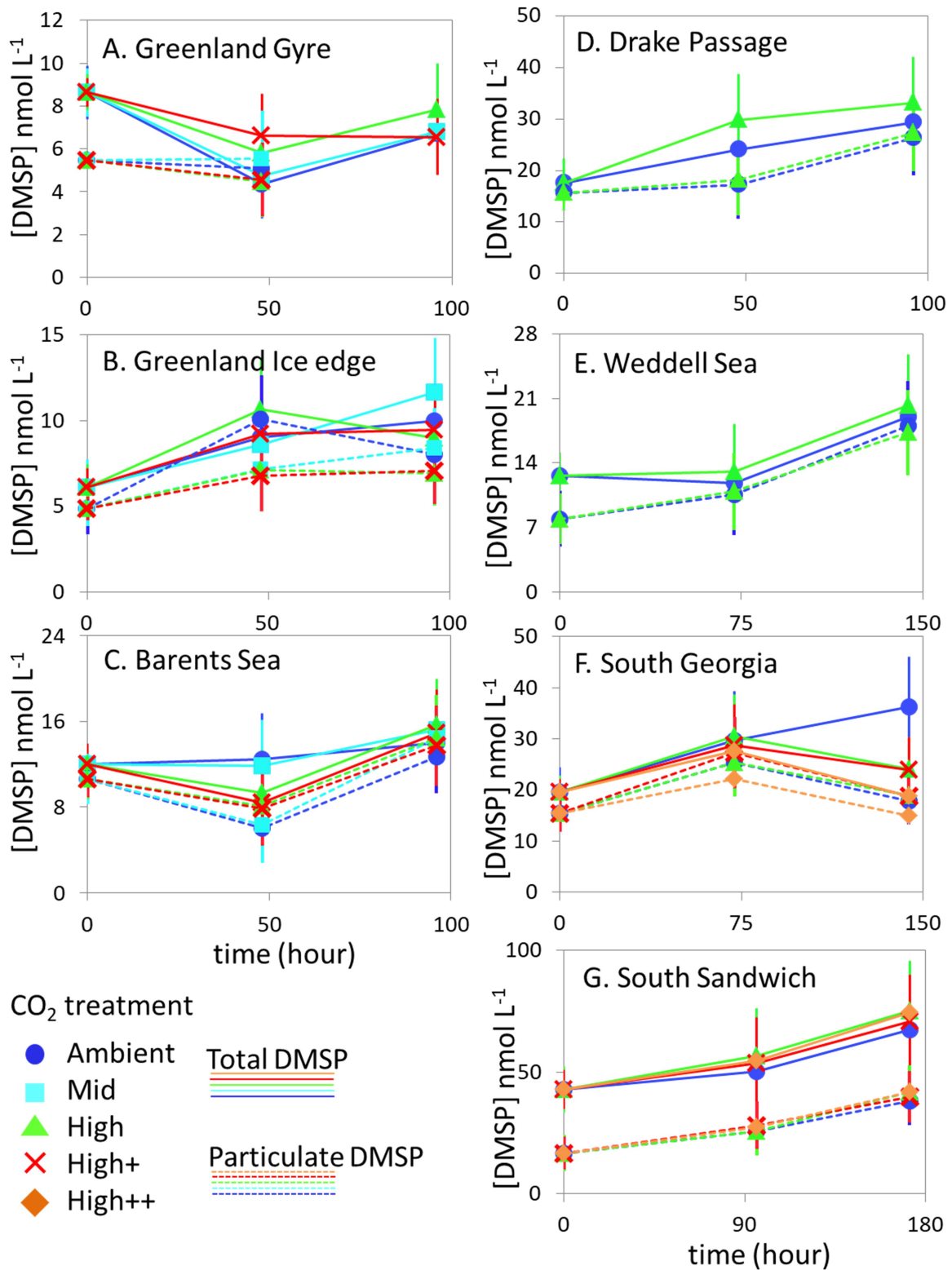
1227 Figure 3. DMS concentrations (nmol L⁻¹) during experimental microcosms performed in
 1228 Arctic waters. Data shown is mean of triplicate incubations, and error bars show standard
 1229 error on the mean. Tables show measurements of pCO₂ (μatm) for each treatment at each
 1230 sampling time point. Initial measurements (0 h) were from a single sample, whilst
 1231 measurements at 48 h and 96 h show mean ± SD of triplicate experimental bottles. Locations
 1232 of water collection for microcosms shown in Figure 1 C – F.



1233

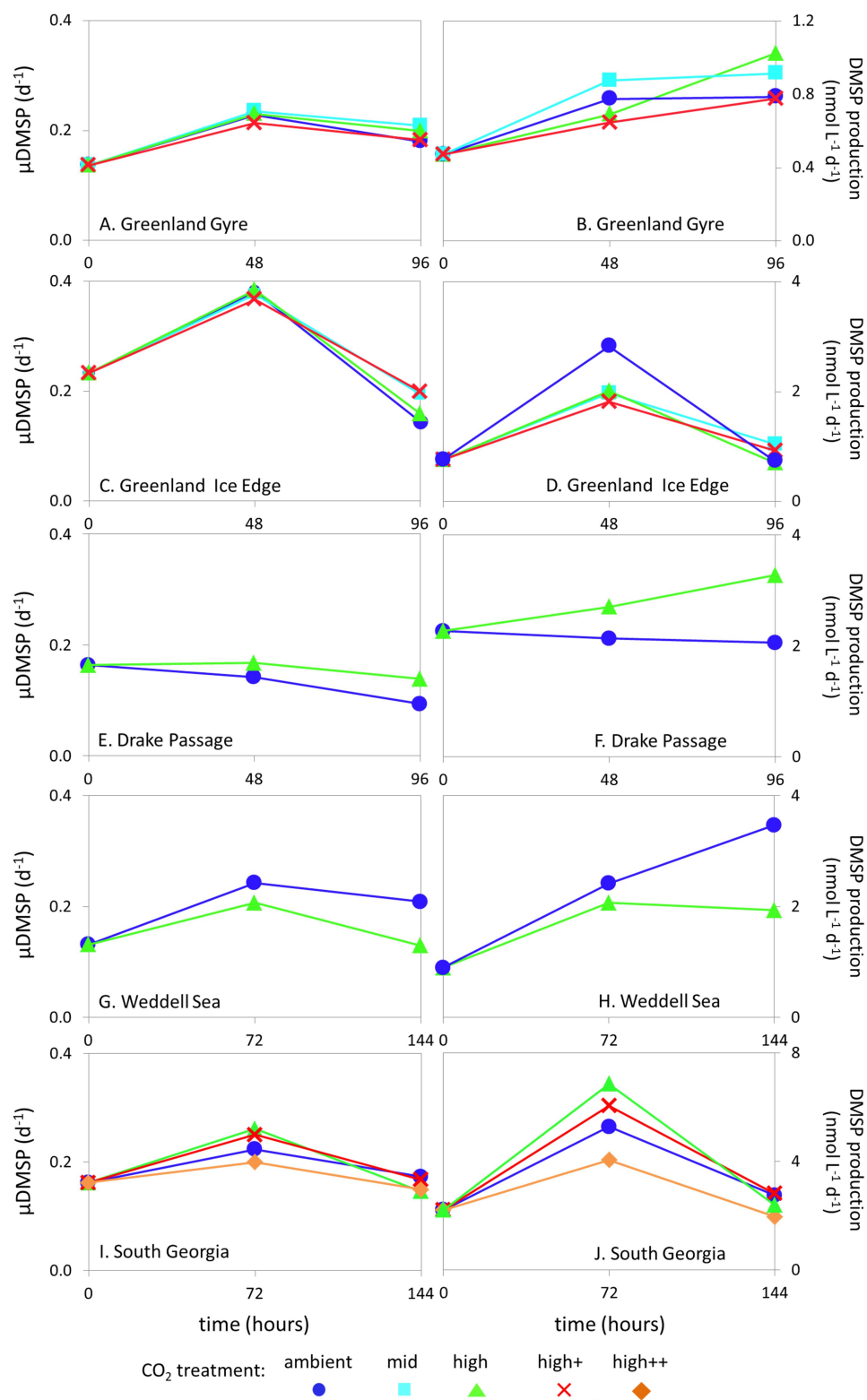
1234 Figure 4. DMS concentrations (nmol L⁻¹) during experimental microcosms performed in
 1235 Southern Ocean waters. Data shown is mean of triplicate incubations, and error bars show
 1236 standard error on the mean. Tables show measurements of pCO₂ (µatm) for each treatment at
 1237 each sampling time point. Initial measurements (0 h) were from a single sample, whilst
 1238 measurements at 48 h and 96 h show mean ± SD of triplicate experimental bottles. Locations
 1239 of water collection for microcosms shown in Figure 1 C – F.

1240



1241

1242 Figure 5. Total DMSP (solid lines) and particulate DMSP (dashed lines) concentrations (
 1243 nmol L⁻¹) during experimental microcosms performed in Arctic waters (A - C) and in
 1244 Southern Ocean waters (D - G). Data shown is mean of triplicate incubations, and error bars
 1245 show standard error on the mean. Locations of water collection for microcosms shown in
 1246 Figure 1 C - F. Particulate DMSP concentrations were used in calculations of DMSP
 1247 production rates (Figure 6).



1249

1250

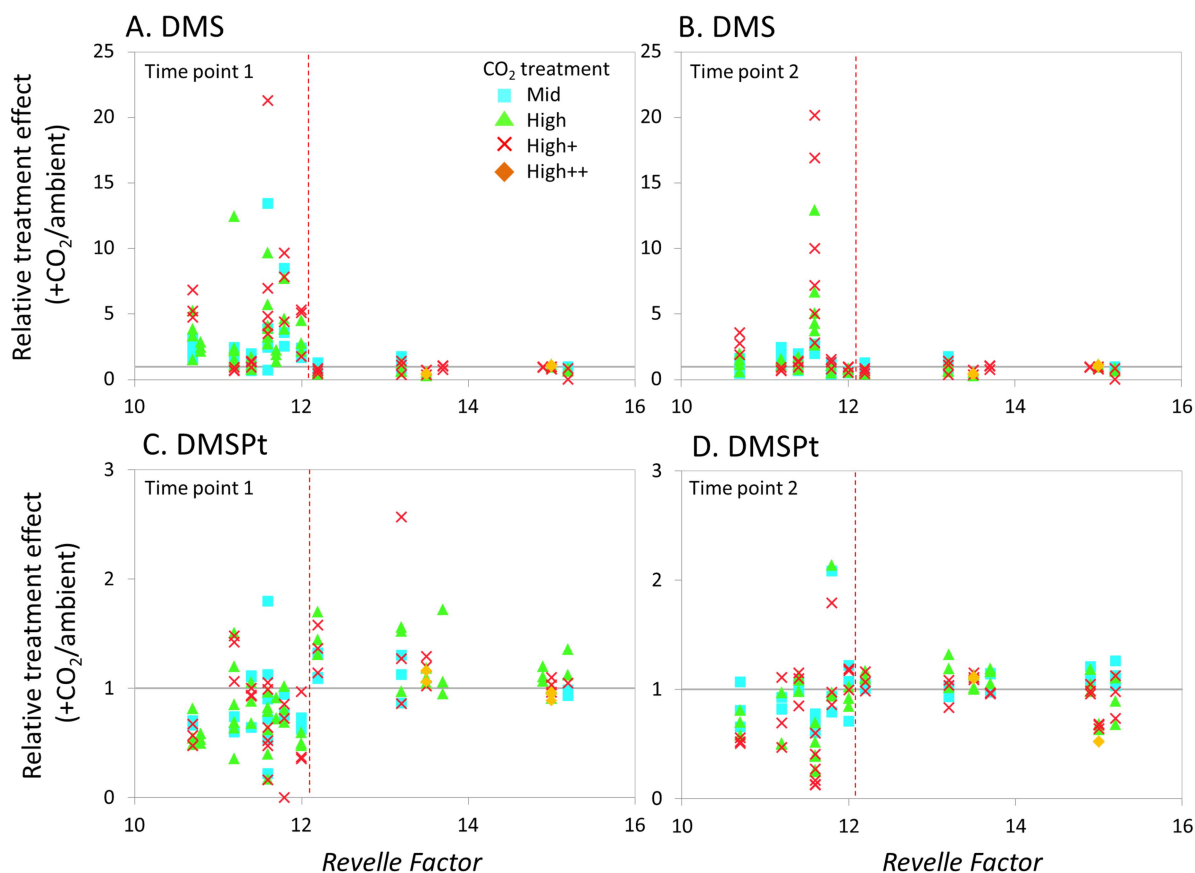
1251

1252

1253

1254

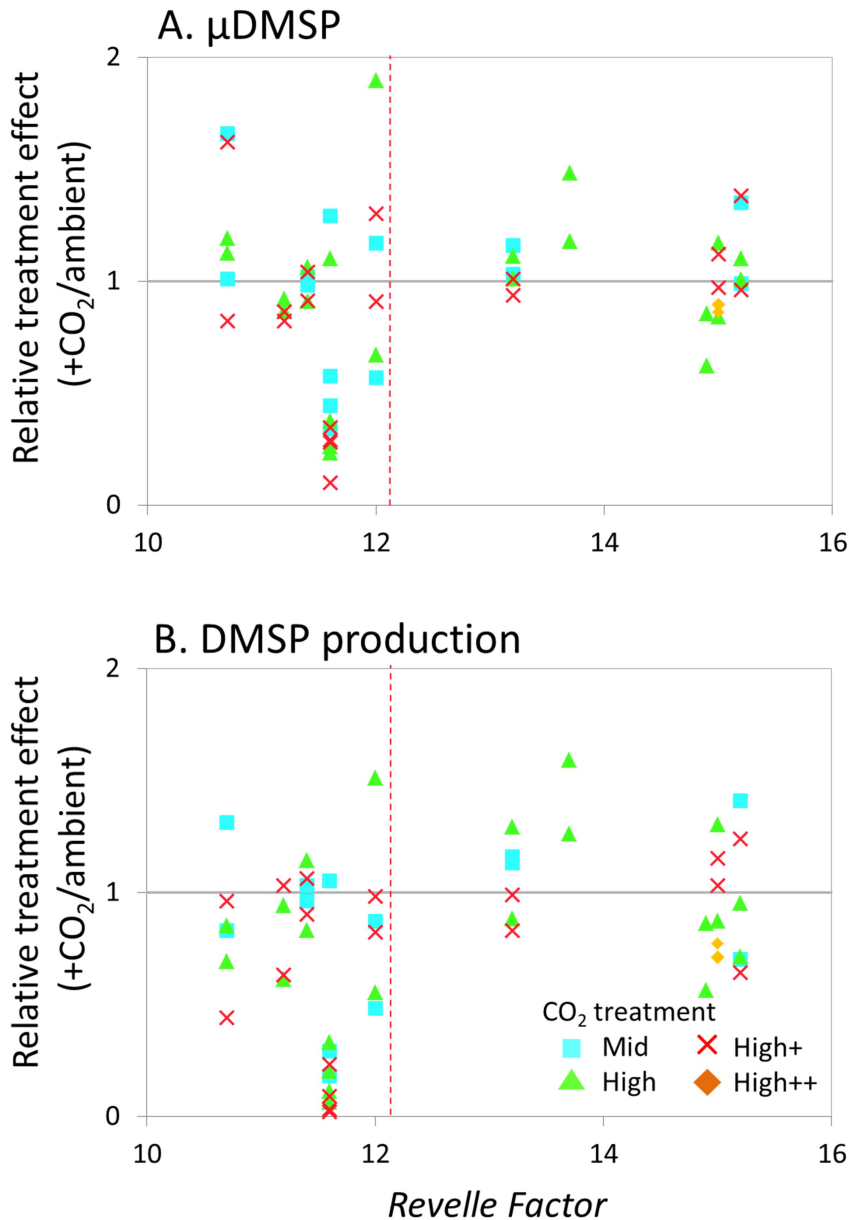
Figure 6. De novo synthesis of DMSP (μDMSP , d^{-1}) (left column) and DMSP production rates ($\text{nmol L}^{-1} \text{d}^{-1}$) (right column) for Arctic Ocean stations *Greenland Gyre* (A,B), *Greenland Ice-edge* (C, D) and Southern Ocean stations *Drake Passage* (E, F), *Weddell Sea* (G, H) and *South Georgia* (I, J). No data is available for *Barents Sea* (Arctic Ocean) or *South Sandwich* (Southern Ocean).



1256

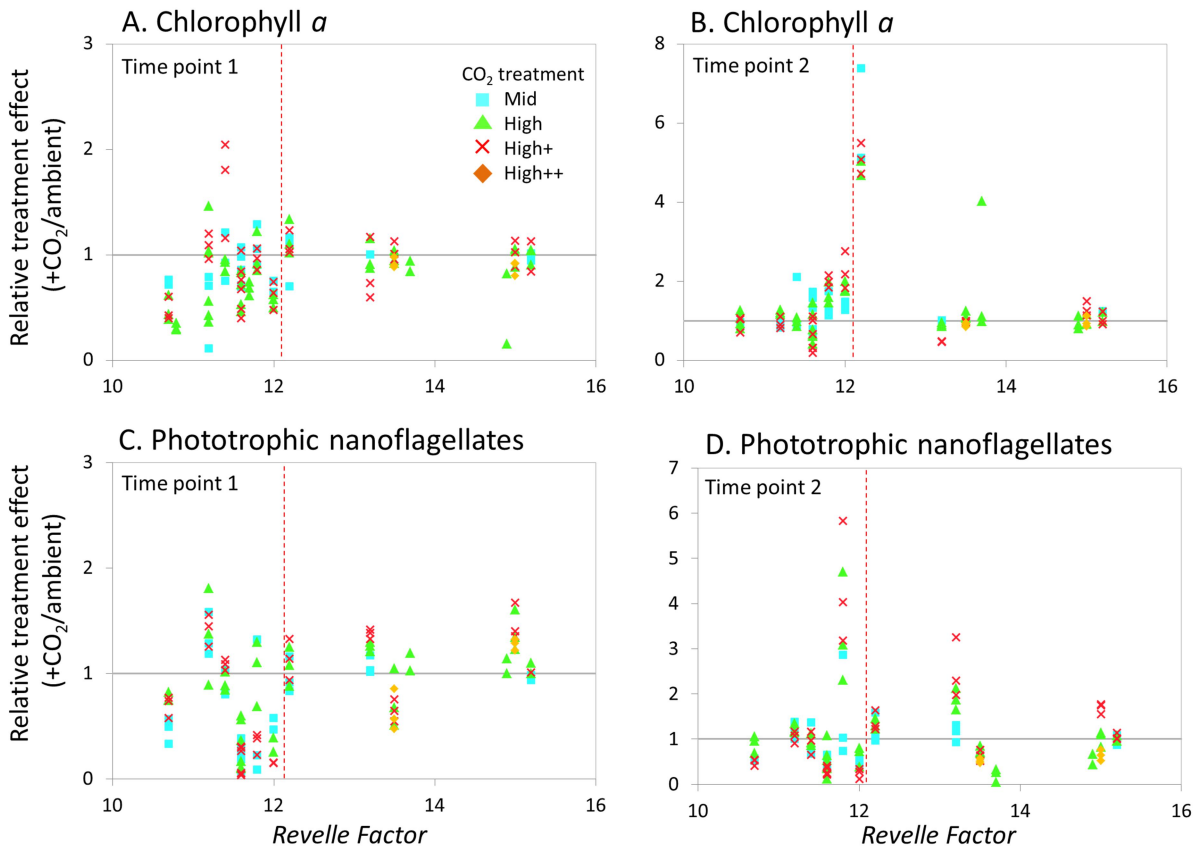
1257 Figure 7. Relationship between Revelle Factor of the sampled water and the relative CO₂
 1258 treatment effect at ($[x]_{\text{highCO}_2}/[x]_{\text{ambientCO}_2}$) for concentrations of DMS at T₁ (A) and T₂ (B),
 1259 and for total DMSPt concentrations at T₁ (C) and T₂ (D) for all microcosm experiments
 1260 performed in NW European waters, sub-Arctic and Arctic waters, and the Southern Ocean.
 1261 Grey solid line (= 1) indicates no effect of elevated CO₂. Revelle Factor > 12 = polar waters
 1262 (indicated by red dashed line). T₁ = 48 h, except for WS and SG (72 h) and SS (96 h). For
 1263 detailed analyses of the NW European shelf data, see Hopkins & Archer (2014).

1264



1265

1266 Figure 8. Relationship between the Revelle Factor of the sampled water and the relative CO₂
 1267 treatment effect at ($[x]_{\text{highCO}_2}/[x]_{\text{ambientCO}_2}$) for de novo DMSP synthesis (μDMSP , d^{-1}) at T₁
 1268 (A) and T₂ (B), and DMSP production rate ($\text{nmol L}^{-1} \text{d}^{-1}$) at T₁ (C) and T₂ (D) for microcosm
 1269 experiments performed in NW European waters, sub-Arctic and Arctic waters, and the
 1270 Southern Ocean. Grey solid line (= 1) indicates no effect of elevated CO₂. Revelle Factor >12
 1271 = polar waters (indicated by red dashed line). T₁ = 48 h, T₂ = 96 h, except for *Weddell Sea*
 1272 and *South Georgia* (72 h, 144 h). For discussion of the NW European shelf data, see Hopkins
 1273 & Archer (2014).



1274

1275 Figure 9. Relationship between the Revelle Factor of the sampled water and the relative CO₂
 1276 treatment effect ($[x]_{\text{highCO}_2}/[x]_{\text{ambientCO}_2}$) for chlorophyll *a* concentrations at T₁ (A) and T₂ (B)
 1277 and phototrophic nanoflagellate abundance at T₁ (C) and T₂ (D) for all microcosm
 1278 experiments performed in NW European waters, sub-Arctic and Arctic waters, and the
 1279 Southern Ocean. Grey solid line (= 1) indicates no effect of elevated CO₂. Revelle Factor >12
 1280 = polar waters (indicated by red dashed line). T₁ = 48 h, T₂ = 96 h, except for *Weddell Sea*
 1281 and *South Georgia* (72 h, 144 h) and *South Sandwich* (96 h, 168 h).

1282

1283

1284